

Spatial distribution of environmental indicators in surface sediments of Lake Bolshoe Toko, Yakutia, Russia

Boris K. Biskaborn^{1*}, Larisa Nazarova^{1,2,3}, Lyudmila A. Pestryakova⁴, Liudmila Syrykh⁵, Kim Funck^{1,6}, Hanno Meyer¹, Bernhard Chaplignin¹, Stuart Vyse¹, Ruslan Gorodnichev⁴, Evgenii Zakharov^{4,7}, Rong Wang⁸, Georg Schwamborn^{1,9}, Hannah L. Bailey¹⁰, Bernhard Diekmann^{1,2}

*Corresponding author's Email: boris.biskaborn@awi.de

1 Alfred Wegener Institute Helmholtz Centre for Polar and Marine Research, Potsdam, Germany

2 University of Potsdam, Potsdam, Germany

3 Kazan Federal University

4 North-Eastern Federal University of Yakutsk, Russia

5 Herzen State Pedagogical University of Russia, St. Petersburg, Russia

6 Humboldt University Berlin, Germany

7 Institute for Biological Problems of Cryolithozone Siberian Branch of RAS, Yakutsk, Russia

8 Key Laboratory of Submarine Geosciences, State Oceanic Administration, Hangzhou, China

9 Free University of Berlin, Berlin, Germany

10 University of Oulu, Ecology and Genetics Research Unit, Oulu, Finland

Manuscript status:

Approved by all authors. English proofread.

Keywords:

Diatoms, chironomids, XRF elements, XRD minerals, grain-size distribution, oxygen isotopes, organic carbon

Abstract

Rapidly changing climate in the northern hemisphere and associated socio-economic impacts require reliable understanding of lake systems as important freshwater resources and sensitive sentinels of environmental change. To better understand time-series data in lake sediment cores it is necessary to gain information on within-lake spatial variabilities of environmental indicator data. Therefore, we retrieved a set of 38 samples from the sediment surface along spatial habitat gradients in the boreal, deep, and yet pristine Lake Bolshoe Toko in southern Yakutia, Russia. Our methods comprise laboratory analyses of the sediments for multiple proxy parameters including diatom and chironomid taxonomy, oxygen isotopes from diatom silica, grain size distributions, elemental compositions (XRF), organic carbon content, and mineralogy (XRD). We analysed the lake water for cations, anions and isotopes. Our results show that the diatom assemblages are strongly influenced by water depth and dominated by planktonic species, i.e. *Pliocaenicus bolshetokoensis*.

44 Species richness and diversity is higher in the northern part of the lake basin,
45 associated with the availability of benthic, i.e. periphytic, niches in shallower waters.
46 $\delta^{18}\text{O}_{\text{diatom}}$ values are higher in the deeper south-western part of the lake probably
47 related to water temperature differences. The highest amount of the chironomid taxa
48 underrepresented in the training set used for palaeoclimate inference was found close
49 to the Utuk river and at southern littoral and profundal sites. Abiotic sediment
50 components are not symmetrically distributed in the lake basin but vary along
51 restricted areas of differential environmental forcing. Grain size and organic matter is
52 mainly controlled by both, river input and water depth. Mineral (XRD) data
53 distributions are influenced by the metamorphic lithology of the Stanovoy mountain
54 range, while elements (XRF) are intermingled due to catchment and diagenetic
55 differences. We conclude that the lake represents a valuable archive for multiproxy
56 environmental reconstruction based on diatoms (including oxygen isotopes),
57 chironomids and sediment-geochemical parameters. **Our analyses suggest multiple**
58 **coring locations preferably at intermediate depth in the northern basin and the deep**
59 **part in the central basin, to account for representative bioindicator distributions and**
60 **higher temporal resolution, respectively.**

61
62

63 **1 Introduction**

64 Over the past few decades, the atmosphere in boreal and high elevation regions
65 has warmed faster than anywhere else on Earth (Pepin et al., 2015;Huang et al.,
66 2017). Dramatic socio-economic and ecological consequences are expected (AMAP,
67 2017) as well as substantial feedbacks from thawing permafrost and the associated
68 release of greenhouse gas into the global climate system (Schuur et al., 2015). Boreal
69 Russia is identified as a global hot-spot where surface air temperature increases have
70 led to substantial ground warming over the past decade (Biskaborn et al., 2019).
71 Accurate estimates of the amplitude of environmental impacts are compounded by an
72 imprecise understanding of ecological indicators of past environmental conditions
73 (Miller et al., 2010). Lake ecosystems, whose development is archived in their
74 sediments, act as sensitive sentinels of environmental changes (Adrian et al., 2009)
75 while even small changes in climate can profoundly deteriorate ecosystem services
76 (Saulnier-Talbot et al., 2014). Assessments of the impact of climate change to lake
77 systems rely on careful interpretation of suitable proxy data. Proxy information on
78 present and past ecological conditions is provided by various biological and
79 physicochemical properties of the sediment components (Meyer et al.,
80 2015;Solovieva et al., 2015;Nazarova et al., 2017a). However, the spatial within-lake
81 distributions of preserved remnants of ecosystem inhabitants and associated
82 sediment-geochemical properties, depend on habitat differences between the

83 epilimnion and the hypolimnion (Raposeiro et al., 2018), and are therefore expected
84 to be non-uniform. Accordingly, precise palaeolimnological reconstruction of past
85 environmental variability requires a detailed, quantitative understanding of the
86 modern (21st century) within-lake heterogeneity.

87 Here, we employ a multi-proxy approach to attain a holistic view of a lake's
88 depositional history in boreal Russia. Variables include diatom and chironomid
89 taxonomy, stable oxygen isotopes in diatom silica, grain size distributions, elemental
90 compositions, organic carbon content, and mineralogy. Abiotic sediment properties
91 may represent signals resulting from either the external input of material and lake-
92 internal conditions during deposition, or post-sedimentary diagenetic processes near
93 the sediment surface (Biskaborn et al., 2013b; Bouchard et al., 2016). Hence, our
94 integrated approach enables the identification and distinction between internal lake
95 processes and external forcing (Cohen, 2003).

96 Diatoms (unicellular, siliceous microalgae) are major aquatic primary producers.
97 They appear ubiquitous and their opaline frustules ($\text{SiO}_2 \cdot n\text{H}_2\text{O}$) are well preserved in
98 the sedimentary record, allowing exact identification down to sub-species level by
99 high-resolution light microscope analysis (Battarbee et al., 2001). Diatoms are widely
100 applied bioindicators for past and present ecosystem changes in boreal environments
101 (Miller et al., 2010; Pestryakova et al., 2012; Hoff et al., 2015; Herzsuh et al.,
102 2013; Biskaborn et al., 2012; Biskaborn et al., 2016; Palagushkina et al., 2017; Douglas
103 and Smol, 2010). Widespread responses of planktonic diatoms to recent climate
104 change indicate that lakes in the northern hemisphere have already crossed important
105 ecological thresholds (Smol and Douglas, 2007; Rühland et al., 2008). The very rapid
106 cell life cycles of days to weeks (Round et al., 1990) enables changes in diatom
107 assemblages on very short time-scales in response to changes in environmental
108 circumstances, e.g. cooling or warming (Anderson, 1990). The link between climate
109 change and diatoms, however, cannot easily be addressed via simple temperature-
110 inference models and instead requires a more complete understanding of the
111 interactions between the aquatic ecosystem with lake habitat preferences,
112 hydrodynamics and catchment properties (Anderson, 2000; Palagushkina et al.,
113 2012; Biskaborn et al., 2016; Bracht-Flyr and Fritz, 2012; Hoff et al., 2015). It is thus
114 necessary to identify the relationship between diatom species occurrence, the
115 isotopic composition of their opaline valves, and internal physico-limnological factors
116 (Heinecke et al., 2017) within spatial heterogenic lake systems before drawing direct
117 inferences about external climatic driven factors from single core studies.

118 Chironomid larvae (Insecta: Diptera) make up to 90% of the aquatic secondary
119 production (Herren et al., 2017; Nazarova et al., 2004) and hence their preserved head
120 capsules well represent the aquatic heterotrophic bottom-dwelling ecosystem
121 component (Nazarova et al., 2008; Syrykh et al., 2017; Brooks et al., 2007).
122 Furthermore, literature reports a net mutualism of chironomids and benthic algae

123 between the primary consumer and primary producer trophic levels in benthic
124 ecosystems (Specziar et al., 2018;Zinchenko et al., 2014). Factors influencing the
125 spatial distribution of chironomids within single lakes are water temperature
126 (Nazarova et al., 2011;Luoto and Ojala, 2018), sedimentological habitat
127 characteristics (Heling et al., 2018) and/or water depth and nutrients (Yang et al.,
128 2017), as well as hypolimnetic oxygen (Stief et al., 2005) and the availability of water
129 plants (Raposeiro et al., 2018;Wang et al., 2012b).

130 As previous studies described, pollen distribution in lake sediments are less
131 influenced by lake zonation than aquatic communities (Zhao et al., 2006).
132 Accordingly, our study does not consider spatial pollen distributions.

133 Secondary factors influencing the spatial distribution of subfossil assemblages are
134 selective transitions from living communities to accumulation of dead remains. Both
135 biological remains and physico-chemical properties are influenced by sediment
136 resuspension and redistribution processes described as sediment focusing (Hilton et
137 al., 1986). These are primarily dependent on slope steepness (Hakanson, 1977) or,
138 in shallow areas, wind-induced bottom shear stress (Bennion et al., 2010;Yang et al.,
139 2009). Nevertheless, it already has been proven for other lake sites that within-lake
140 bioindicator distributions are laterally non-uniform, contradicting the assumption that
141 mixing processes cause homogenous microfossil assemblages before deposition
142 (Anderson, 1990;Wolfe, 1996;Anderson et al., 1994;Earle et al., 1988;Kingston et al.,
143 1983;Puusepp and Punning, 2011;Stewart and Lamoureux, 2012;Yang et al., 2009).
144 However, many palaeolimnological studies employ single-site approaches using only
145 one sediment core, and hence do not encompass the full spatial extent and natural
146 variability of the entire lake sediment archive. Heggen et al. (2012) report that
147 sediment cores from the deep centre of small and shallow lakes with high spatial
148 proxy variability in the littoral zones contain representative bioindicator assemblages.
149 The authors also conclude, that in larger and deeper lakes similar multi-site studies
150 are necessary to make recommendations about the “ideal” coring positions for multi-
151 proxy palaeolimnological studies.

152 In this respect, our broad research question is: how spatially reliable are
153 palaeolimnological proxy data in a complex lake system? To answer this question, we
154 set up our research hypothesis: Bioindicators and abiotic sediment properties will
155 respond to different habitat conditions and lake zonation, including water depth,
156 proximity to the main inflow in the South and old moraines in the North of lake Bolshoe
157 Toko.

158 An analysis of spatio-temporal within-lake bioindicator distribution requires a
159 suitable and large lake system with an anthropogenically untouched ecosystem and
160 sufficient variability in water depth, catchment setting, and sedimentological regime.
161 These demands are met by Lake Bolshoe Toko, the deepest lake in Yakutia, Russia
162 (Zhirkov et al., 2016) (Fig. 1). Our study aims to gain a better local understanding of

163 proxy data for future palaeoenvironmental analyses of long sediment cores from
164 Bolshoe Toko. Therefore, our objectives are to (1) detect the spatial variability of
165 abiotic (elements, minerals, grain size) and biotic (diatoms, chironomids, organic
166 carbon) components of the lake's surface sediments, (2) reveal the causal
167 relationship between the distribution of aquatic microfossils, lake basin features, and
168 sedimentary parameters, and (3) attribute proxy variability to specific environmental
169 factors.

170

171 **2 Study site**

172 Lake Bolshoe Toko (56°15'N, 130°30'E, 903 m.a.s.l) is an oligotrophic, freshwater
173 lake located in the Sakha Republic, Russia (Fig. 1). The lake surface area is 84.3
174 km², with a mean water depth of 29.5 m (maximum, 72.5 m) and secchi depth of 9.8
175 m (Zhirkov et al., 2016). The Utuk river runs through Lake Maloe Toko and brings
176 water from the southern igneous catchment. Lake Maloe Toko (called "small Toko",
177 size 2.7 x 0.9 km, 168 m depth, tectonic origin) is located between high mountains
178 south of Bolshoe Toko. The river inflow south of Bolshoe Toko forms deltaic
179 sediments. The bay in the southeast is called Zaliv Rybachiyy ("Fishing bay"). It is
180 partly separated from the main basin and supplied with water by a small creek that
181 itself is connected to a small lake (Fig. 1). The bay is reported to have a somewhat
182 different fauna as compared to the Bolshoe Toko main basin, i.e. occurrence of fish
183 that are typical for small lakes and not found out of the basin (Semenov, 2018). The
184 "Banya lake" in the northeast is isolated from Bolshoe Toko and is not considered in
185 this study. The Mulam river is the lake's predominant outflow towards the North along
186 the south eastern border of Yakutia flowing into the Uchur, Aldan and finally into the
187 Lena rivers.

188 There are no permanent settlements in the study area. During the time of field work
189 there was a temporary mining settlement (built in 2011) located 17 km northwest from
190 Bolshoe Toko in the upper course of the Elga river. This settlement was accessible
191 by off-road vehicles we used to reach the lake, partly along temporary winter roads
192 (frozen rivers and lakes) in March 2013. The exploitation of the El'ginsky coal
193 deposits, planned for a productivity of 15-20 million tons year⁻¹ (Konstantinov, 2000),
194 will strongly affect the lake and its catchment. The territory of the watershed will
195 increasingly be damaged and contaminated by off road vehicles and rain fall will
196 produce muddy water which potentially can cause lake pollution (Sobakina and
197 Solomonov, 2013).

198 The lake basin is adjoined to the northern slope of the eastern Stanovoy mountain
199 range in a depression of tectonic and glacial origin between two northwest-trending
200 right-lateral strike-slip faults (Imaeva et al., 2009). A southward thrust fault runs along
201 the southern border of the lake separating the Precambrian igneous rocks in the south

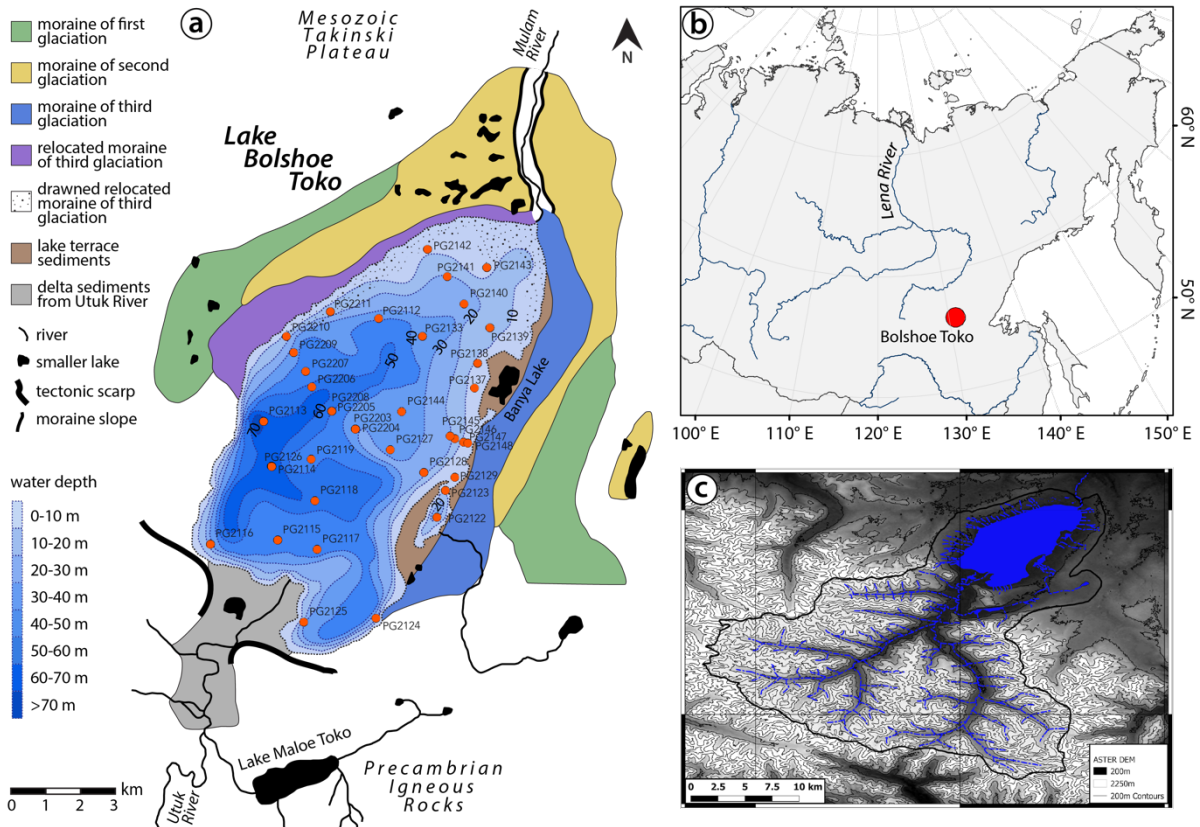
202 from sandstones and mudstones of the Mesozoic Tokinski Plateau in the north. The
203 Stanovoy mountain range in the southern catchment of the lake consists mainly of
204 highly mafic granulites and other high-pressure metamorphic rock types (Rundqvist
205 and Mitrofanov, 1993). At its north-eastern margins the lake is bordered by moraines
206 of three different glacial sub-periods (Kornilov, 1962) (Fig. 1).

207 The study area is situated within the East Siberian continental temperate climate
208 zone exhibiting taiga vegetation (boreal forests) and fragments of steppes and a
209 predominant westerly wind system (Shahgedanova, 2002). The meteorological
210 station in Yakutsk has recorded historical climate data (Gavrilova, 1993). In the 19th
211 Century the mean annual temperature (Jan-Dec) was circa -11° to -11.5°C and during
212 the 20th Century these temperatures have increased to around -10.2°C, in parallel
213 with an increase in precipitation from 205 to 250 mm per year (Konstantinov, 2000).
214 The meteorological station “Toko” located approximately 10 km northeast of the lake,
215 however, recorded an increase of air temperature of ca. 0.48 °C per decade from the
216 1970’s to 2010 (calculated from NOAA data, only those years involved that have
217 average air T data in 12 months). Measurements taken directly at the lake were lower,
218 indicating the influence of cold melt water from the Stanovoy mountain range in
219 summer and the high volume of ice during wintertime. Since the average air
220 temperature in southern Yakutia increases with height (temperature inversion of ~2°C
221 100 m⁻¹), permafrost can be locally discontinuous where taliks (unfrozen zones)
222 underneath topographically high and deep lakes penetrate the permafrost zone
223 (Konstantinov, 1986). As observed in 1971 (Konstantinov, 2000) ice cover lasts at
224 least partly until mid-July.

225

226

227



228
229
230
231
232
233
234
235
236
237

Fig. 1 Lake Bolshoe Toko study site. **a** Geological map, bathymetry and moraines. Map compiled using data from Konstantinov (2000) and Kornilov (1962). **b** Overview map of Siberia. World Borders data are derived from http://thematicmapping.org/downloads/world_borders.php and licensed under CC BY-SA 3.0. **c** Catchment area around Bolshoe Toko delineated from the ASTER GDEM V2 model between the latitudes N54° and N56° and longitudes E130° to E131° (1) (Meyer et al., 2011) and a corresponding multispectral Landsat 8 OLI TIRS satellite image using QGIS (QGIS-Team, 2016). Most of the river catchment is located in the igneous Precambrian Stanovoy mountain range supplying the southern part of the lake with water and sediment. The shallower northeastern part of the lake is influenced by the surrounding moraines and Mesozoic sand- and mudstones.

238 3 Materials and methods

239 3.1 Field work

240 Field work was conducted during the German-Russian expedition “Yakutia 2013”
241 between March 19th to April 14th 2013 by the Alfred Wegener Institute Helmholtz
242 Centre for Polar and Marine Research (AWI) and the North Eastern Federal State
243 University in Yakutsk (NEFU). Vertical holes were drilled in the lake ice cover using a
244 Jiffy ice auger with a diameter of 250 mm. Lake basin bathymetry was measured
245 using a portable Echo Sounder. Ice cores were retrieved by drilling multiple holes
246 around a central part. Water samples for hydrochemical analyses were collected prior
247 to sediment coring using a UWITEC water sampler. Water samples were analysed in
248 situ using a WTW Multilab 340i for pH, conductivity, and oxygen values at the day of
249 retrieval during field work. A sub-sample of the original water was passed through a
250 0.45 µm cellulose-acetate filter, stored and transported in 60-ml Nalgene polyethylene

251 bottles for subsequent anion and cation analyses in AWI laboratories in autumn 2013.
252 Cation samples were acidified during field work with HNO₃, suprapure (65%) to
253 prevent microbial conversion processes and adsorptive accretion.

254 At 42 sites within the lake, short cores containing intact sediment surface material
255 were retrieved using an UWITEC gravity corer. Water depth at sampling sites was
256 measured using either a hand-held HONDEX PS-7 LCD digital sounder and/or the
257 cord of the coring device when the lake ice cover disturbed the signal. The sediment
258 was identified as clayish silt deposits with predominant dark (black) color and a weak
259 smell of hydrogen sulphide, a sticky and viscous mud mixed with plant and other
260 organic residues. The uppermost ca. 2 cm at some sites had a dark red colouring
261 indicating the redox boundary between oxygenated and anoxic sediments. We
262 identified the uppermost 0.5 cm of short cores as surface sediments and subsampled
263 these layers onsite during fieldwork to avoid sediment mixture during transport.
264 Sediment samples were transported in sterile "Whirl-Pak" bags and sediment cores
265 were transported in plastic liners to the AWI laboratories in Potsdam, Germany, and
266 stored at 4°C in a dark room for further analyses and as back-up.

267 **During this expedition also long core material was retrieved from multiple sites**
268 **including the northern and central part of the lake and is planned for publication in a**
269 **separate manuscript.**

270 According to the amount the uppermost 0-0.5 cm layer in the short cores available
271 the sample size n for different sediment properties measured in this study vary.

272 **3.2 Laboratory analyses**

273 **3.2.1 Hydrochemistry**

274 Water depth profiles were taken during the March 2013 expedition from the
275 deepest part of the lake (PG2208, water depth 70m) and in the lagoon (PG2122, 18
276 m) as well as in **August 2012** (sample site near the western shoreline, 37 m). The
277 temperature was determined in the field and the samples analysed for isotopes ($\delta^{18}\text{O}$,
278 δD , see Fig. 6). From the water samples anions were analysed using ion
279 chromatography (Dionex DX 320) and cations were determined using inductively
280 coupled plasma–optical emission spectrometry (ICP-OES, Perkin-Elmer Optima
281 8300DV Perkin-Elmer – Optical Emission Spectrometer. Alkalinity was measured by
282 titration with 0.01 M HCl using an automatic titrator (Metrohm 794 Basic Titrino).

283 Stable hydrogen and oxygen isotope analyses were carried out with Finnigan MAT
284 Delta-S mass spectrometers with two equilibration units using common equilibration
285 techniques (Meyer et al., 2000), and given as $\delta^{18}\text{O}$ and δD in ‰ vs. VSMOW
286 (Vienna Standard Mean Ocean Water) with respective analytical errors of better than
287 $\pm 0.1\%$ and 0.8% . The secondary parameter d-excess (d) is calculated as $d = \delta\text{D} - 8\delta^{18}\text{O}$
288 (^{18}O) (Dansgaard, 1964; Merlivat and Jouzel, 1979).

289 **3.2.2 X-ray fluorescence and X-ray diffractometry**

290 To gain information on the variability of the elemental sediment composition, 20
291 freeze-dried and milled surface samples were semi-quantitatively analysed by X-ray
292 fluorescence (XRF) using a novel single sample modification for the AVAATECH XRF
293 core scanner at AWI Bremerhaven. A Rhodium X-ray tube was warmed up to 1.75mA
294 and 3 mA with a detector count time of 10s and 15s for elemental analysis at 10kV
295 (No filter) and 30kV (Pd-Thin filter) respectively. The average modelled chi square
296 values (χ^2) of measured peak intensity curve fitting for the relevant elements were
297 variable, but generally low (Zr = 0.92, Mn = 1.49, Fe = 2.32, Ti = 1.53, Br = 3.65, Sr =
298 4.79, Rb = 4.98, Si = 16.11). Values above 3 were ascribed to suspiciously high count
299 rates from sample PG2133 which was subsequently excluded from XRF
300 interpretation. The relatively low amount of total sample material available did not
301 facilitate the removal of organic matter prior to sample measurement and may have
302 contributed to the variable modelled chi square values.

303 As interpretation of raw device obtained element intensities (in counts per second,
304 cps) is problematic due to non-linear matrix effects and variations in sample density,
305 water content and grain-size (Tjallingii et al., 2007), cps values were transformed
306 using a centred-log ratio transformation (CLR). Element ratios were calculated from
307 raw cps values and transformed using an additive-log ratio transformation (ALR)
308 (Weltje and Tjallingii, 2008).

309 The mineralogical composition of 32 freeze-dried and milled samples was analysed
310 by standard X-ray diffractometry (XRD) using a Philips PW1820 goniometer at AWI
311 Bremerhaven applying Cobalt-Potassium alpha (CoK α) radiation (40 kV, 40 mA) as
312 outlined in Petschick et al. (1996). The intensity of diffracted radiation was calculated
313 as counts of peak areas using XRD processing software MacDiff 4.0.7 (freeware
314 developed by R. Petschick in 1999). Individual mineral content was expressed as
315 percentages of bulk sediment XRD counts (Voigt, 2009). Mineral inspection focused
316 on quartz, plagioclase and K-feldspar, hornblende, mica, and pyrite. Clay minerals
317 involved kaolinite, smectite and chlorite. Accuracy of the semi-quantitative XRD
318 method is estimated to be between 5 and 10% (Gingele et al., 2001).

319

320 **3.2.3 Grain-size, carbon and nitrogen analyses**

321 In order to gain high-resolution information on the spatial variability of particle sizes
322 and related water energy in the lake, we analysed the grain-size distribution using
323 laser technique. Organic material was removed from 32 surface sediment samples by
324 hydrogen peroxide oxidation over four weeks on a platform shaker. Two homogenised
325 subsamples were weighted and 93 subclasses between 0.375 and 2000 μm were
326 measured using a Coulter LS 200 Laser Diffraction Particle Analyser. Grain-size

327 fractions coarser than 2 mm were sieved out, weighted and added to the volume
328 percentage data afterwards to indicate the proportion of gravel.

329 To assess the accumulation of organic matter in the lake, we analysed total carbon
330 (TC) and total nitrogen (TN) of 35 freeze-dried and milled samples. For TC and TN
331 we quantified bulk samples by heating the material in small tin capsules using a Vario
332 EL III CNS analyser. Total organic carbon (TOC) was measured using a Vario MAX
333 C in per cent by weight (wt%). The measurement accuracy was 0.1 wt% for TOC and
334 TN, and 0.05 wt% for TC. TOC and TN were compared to calculate the TOC/TN_{atomic}
335 ratio by multiplying with the ratio of atomic weights of nitrogen and carbon following
336 Meyers and Teranes (2002).

337 To gain additional bioproductivity information we analysed the stable carbon
338 isotope composition $\delta^{13}\text{C}$ of the total organic carbon fraction in 15 samples using a
339 Finnigan Delta-S mass spectrometer. Dried, milled and carbonate-free (HCl treated)
340 samples were combusted in tin capsules to CO₂. Results are expressed as $\delta^{13}\text{C}$
341 values relative to the PDB standard in parts per thousand (‰) with an error of $\pm 0.15\%$.

342 Radiocarbon dating of two bulk sediment surface sample from short cores, each
343 ranging from 0-0.5 cm depth below the sediment surface, was performed in the
344 Poznan Radiocarbon Laboratory on the soluble (SOL) fraction using an Accelerator
345 Mass Spectrometer.

346

347 **3.2.4 Diatoms**

348 23 samples were prepared for diatom analysis following the standard procedure
349 (Battarbee et al. (2001)). To calculate the diatom valve concentration (DVC) 5×10^6
350 microspheres were added to each sample following organic removal with hydrogen
351 peroxide. Diatom slides were prepared on a hot plate using Naphrax mounting
352 medium. For the identification of diatoms to the lowest possible taxonomic level we
353 used several diatom flora including Lange-Bertalot et al. (2011), Lange-Bertalot and
354 Metzeltin (1996), Krammer and Lange-Bertalot (1986-1991) and Lange-Bertalot and
355 Genkal (1999). For rare taxa (i.e. *Pliocaenicus*) literature research was applied in
356 scientific papers, including Cremer and Van de Vijver (2006) and Genkal et al. (2018).
357 A minimum of 300 (and up to 400) diatom valves were counted in each sample using
358 a Zeiss AXIO Scope.A1 light microscope with a Plan-Apochromat 100 \times /1.4 Oil Ph3
359 objective at 1000x magnification. Identification of small diatom species was verified
360 using a scanning electron microscope (SEM) at the GeoForschungsZentrum
361 Potsdam.

362 During counting of diatom valves, chrysophycean stomatocysts and *Mallomonas*
363 were counted but not further taxonomically identified. Count numbers were used to
364 estimate the chrysophyte cyst to diatom index (C:D) and *Mallomonas* to diatom index
365 (M:D) relative to counted diatom cells (Smol, 1984; Smol and Boucherle, 1985).

366 Diatom valve preservation was measured and calculated as the f-index (Ryves et al.,
367 2001). Diatom valve concentration was estimated as the number of valves per gram
368 dry sediment following Battarbee and Kneen (1982).
369

370 **3.2.5 Oxygen isotopes of diatom silica**

371 To analyze the oxygen isotope composition from diatom silica ($\delta^{18}\text{O}_{\text{diatom}}$) from 9
372 representative surface samples, a purification procedure including wet chemistry (to
373 remove organic matter and carbonates) and heavy liquid separation was applied for
374 the fraction $<10\ \mu\text{m}$ following the method described in Chaplignin et al. (2012a). After
375 freeze-drying the samples were treated with H_2O_2 (32%) and HCl (10%) to remove
376 organic matter and carbonates and wet sieved into $<10\ \mu\text{m}$ and $>10\ \mu\text{m}$ fractions.
377 Four multiple heavy liquid separation (HLS) steps with varying densities (from 2.25 to
378 2.15 g/cm^3) were then applied using a sodium polytungstate (SPT) solution before
379 being exposed to a mixture of HClO_4 (65%) and HNO_3 (65%) for removing any
380 remaining micro-organics.

381 To remove exchangeable hydrous groups from the diatom valve structure
382 (amorphous silica $\text{SiO}_2 \cdot n\text{H}_2\text{O}$), inert Gas Flow Dehydration was performed
383 (Chaplignin et al., 2010). Oxygen isotope analyses were performed on dehydrated
384 samples using laser fluorination technique (with BrF_5 as reagent to liberate O_2) and
385 then directly measured against an oxygen reference of known isotopic composition
386 using a PDZ Europa 2020 mass spectrometer (MS2020, now supplied by Sercon Ltd.,
387 UK). The long-term analytical reproducibility (1σ) is $\pm 0.25\ \text{‰}$ (Chaplignin et al., 2010).

388 Every fifth sample was a biogenic working standard to verify the quality of the
389 analyses. For this, the biogenic working standard BFC calibrated within an inter-
390 laboratory comparison was used (Chaplignin, 2011). With a $\delta^{18}\text{O}$ value of $+29.0 \pm 0.3$
391 ‰ (1σ) BFC (this study: $+28.7 \pm 0.17\ \text{‰}$, $n=49$) is the closest diatom working standard
392 to the Bolshoe Toko samples ($\delta^{18}\text{O}$ values range between $+22$ and $+24\ \text{‰}$) available.
393 A contamination correction was applied to $\delta^{18}\text{O}_{\text{diatom}}$ using a geochemical mass-
394 balance approach (Chaplignin et al., 2012a; Swann et al., 2007) determining the
395 contamination end-member by analysing the heavy fractions after the first heavy liquid
396 separation resulting in $\text{Al}_2\text{O}_3=16.2 \pm 1.3\ \%$ (via EDX; $n=9$) and $\delta^{18}\text{O}=8.5 \pm 0.8\ \text{‰}$ ($n=6$).

397 **3.2.6 Chironomids**

398 Treatment of 18 sediment samples for chironomid analysis followed standard
399 techniques described in Brooks et al. (2007). Subsamples of wet sediments were
400 deflocculated in 10 % KOH , heated to $70\ \text{°C}$ for up to 10 minutes, to which boiling
401 water was added and left to stand for up to another 20 minutes. The sediment was
402 passed through stacked 225 and $90\ \mu\text{m}$ sieves. Chironomid larval head capsules
403 were picked out of a grooved Bogorov sorting tray under a stereomicroscope at 25-

404 40x magnifications and were mounted in Hydromatrix two at a time, ventral side up,
405 under a 6 mm diameter cover slip. From 48 to 117 chironomid larval head capsules
406 were extracted from each sample, to capture the maximum diversity of the chironomid
407 population. Chironomids were identified to the highest taxonomic resolution possible
408 with reference to Wiederholm (1983) and Brooks et al. (2007). Information on the
409 ecology of chironomid taxa and groups was taken from Brooks et al. (2007), Pillot
410 (2009) and Nazarova et al., (2011;2015;2008;2017b)). Ecological information of the
411 taxa associated to biotopes (littoral, profundal), water velocity (standing, running
412 water), and relation to presence of macrophytes were taken from Brooks et al. (2007)
413 and Pillot (2009). T July optima of chironomids were taken from Far East (FE)
414 chironomid-based temperature inference model (Nazarova et al., 2015). The Far East
415 (FE) chironomid-based temperature inference model (WA-PLS, 2 components; r^2
416 boot = 0.81; RMSEP boot = 1.43 °C) was established from a modern calibration data
417 set of 88 lakes and 135 taxa from the Russian Far East (53–75°N, 141–163°E, T July
418 range 1.8 – 13.3 °C). Mean July air temperature for the lakes from the calibration data
419 set was derived from New et al. (2002). All modern and chironomid-inferred
420 temperatures were corrected to 0 m.a.s.l. using a modern July air temperature lapse
421 rate of 6 °C km⁻¹ (Livingstone et al., 1999;Heiri et al., 2014).

422 **3.3 Statistical analyses**

423 Detrended Correspondence Analysis (DCA) with detrending by segments was
424 performed on the chironomid and diatom data (rare taxa downweighted) to determine
425 the lengths of the sampled environmental gradients, from which we decided whether
426 unimodal or linear statistical techniques would be the most appropriate for the data
427 analysis (Birks, 1995). For diatom data the gradient lengths of the species scores
428 were 2.07 and 1.49 standard deviation units (SDU) for DCA 1 and 2, respectively,
429 suggesting that lineal numerical methods should be used. A Principal Component
430 Analysis (PCA) was used to explore the main taxonomic variation of the data (ter
431 Braak and Prentice, 1988). The gradient lengths of chironomid species scores were
432 3.78 and 4.12 SDU indicating that numerical methods based on a unimodal response
433 model should be more appropriate to assess the variation structure of the chironomid
434 assemblages (ter Braak, 1995). However, test PCA performed on chironomid data
435 showed that lineal method captures more variance of species data (ESM, Table 2)
436 therefore we further applied lineal methods for both, chironomid and diatom data. In
437 order to summarize the response of lacustrine biota to abiotic, physicochemical
438 explanatory variables, a redundancy analysis (RDA) was performed on diatom and
439 chironomid data in comparison to environmental variables (Fig. 2 and 3).

440 Initially, all environmental variables shown in this paper were tested in a RDA to
441 assess the relationships between the distribution of bioindicator taxa and abiotic
442 habitat parameters. Apart from the chemical and physical parameters of the lake and

443 sediments (Fig. 5), we include in the analysis the presence/absence of the submerged
444 vegetation, distances of the sampling stations from the shore and from the inflowing
445 rivers. All explanatory variables were tested for normality prior to the analyses.
446 Skewness reflects the degree of asymmetry of a distribution around its mean. Normal
447 distributions produce a skewness statistic of about zero. Values that exceeded 2
448 standard errors of skewness were identified as significantly skewed (Sokal and Rohlf,
449 1995). Environmental variables with skewed distributions (gravel, grain-size EM2,
450 smectite-chlorite, mica, K-feldspar) were log transformed and remaining parameters
451 were left untransformed. To reveal intercorrelated parameters, we performed a
452 variance inflation factor (VIF) analysis prior to ordination techniques to only retain
453 non-correlated parameters in further multivariate analysis. Environmental variables
454 with a VIF greater than 20 were eliminated, beginning with the variable with the largest
455 inflation factor, until all remaining variables had values < 20 (ter Braak and Smilauer,
456 2012). A set of RDAs was performed on chironomid and diatom data with each
457 environmental variable as the sole constraining variable. The percentage of the
458 variance explained by each variable was calculated and statistical significance of
459 each variable was tested by a Monte Carlo permutation test with 999 unrestricted
460 permutations. Significant variables ($P \leq 0.05$) were retained for further analysis. DCA,
461 PCA and RDA were performed using CANOCO 5.04 (ter Braak and Smilauer, 2012).

462 Percentage abundances of the chironomid taxa that are absent or rare in the
463 modern calibration data set were calculated at each sampling site in order to see the
464 distribution of the taxa that could potentially hamper a T July reconstruction in case
465 of palaeoclimatic study that could be done at each of the sampling sites. It is known
466 that less reliability should be placed on the samples in which more than 5% of the
467 taxa are not represented in the modern calibration data or more than 5% of the taxa
468 are rare in the modern calibration dataset (i.e., if the effective number of occurrences
469 in the training set, the Hill's N2, is less than 5) (Heiri and Lotter, 2001; Hill, 1973; Self
470 et al., 2011).

471 Species richness and the Simpson diversity on diatom and chironomid data were
472 estimated after sample-size normalization using a rarefaction analysis of Hill numbers
473 in the iNEXT package in R.

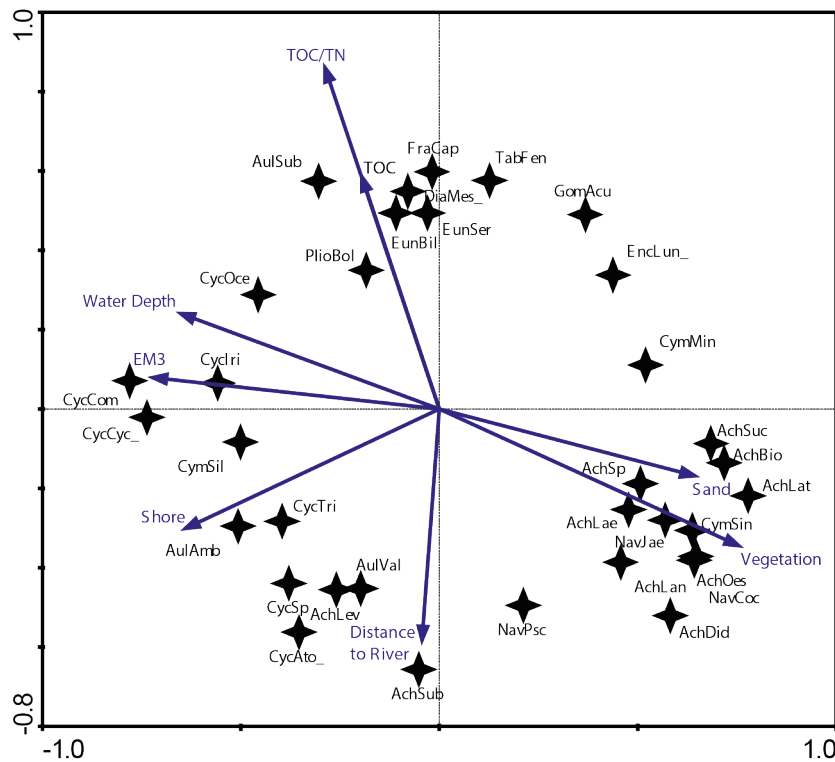
474 To assess the relative contribution of different sedimentary processes to the bulk
475 sediment, such as fluvial or aeolian transport (Wang et al., 2015; Biskaborn et al.,
476 2013b) a statistical end-member analysis on grain-size data was performed using the
477 MATLAB modelling algorithm of Dietze et al. (2012). In this method, individual grain-
478 size populations identified as end-member loadings (vol%, Fig. 4) as well as their
479 contributions to the bulk composition identified as scores (%) were derived by
480 eigenspace analysis, weight transformation, varimax rotations and different scaling
481 procedures.

482 A Pearson correlation matrix of the main important variables (Fig. 5a) was
483 calculated using the basic R core (R Core Team, 2012) and plotted using *corrplot*. To
484 keep false discovery rate below 5% a p-value adjustment was applied prior to
485 assignment of colours using only values that revealed $p < 0.001$ (Colquhoun, 2014).
486 To identify the pattern, the correlation matrix was reordered according to the
487 correlation coefficient. Exceptional sites within the heterogenic lake system lead to
488 disturbance of good correlation coefficients within areas along natural borders, e.g.
489 water depth isobaths. Spatial autocorrelation of variables was estimated using
490 latitudes and longitudes recorded of each sample site and displayed as p values
491 generated by Moran's Autocorrelation Coefficient (R package "ape").

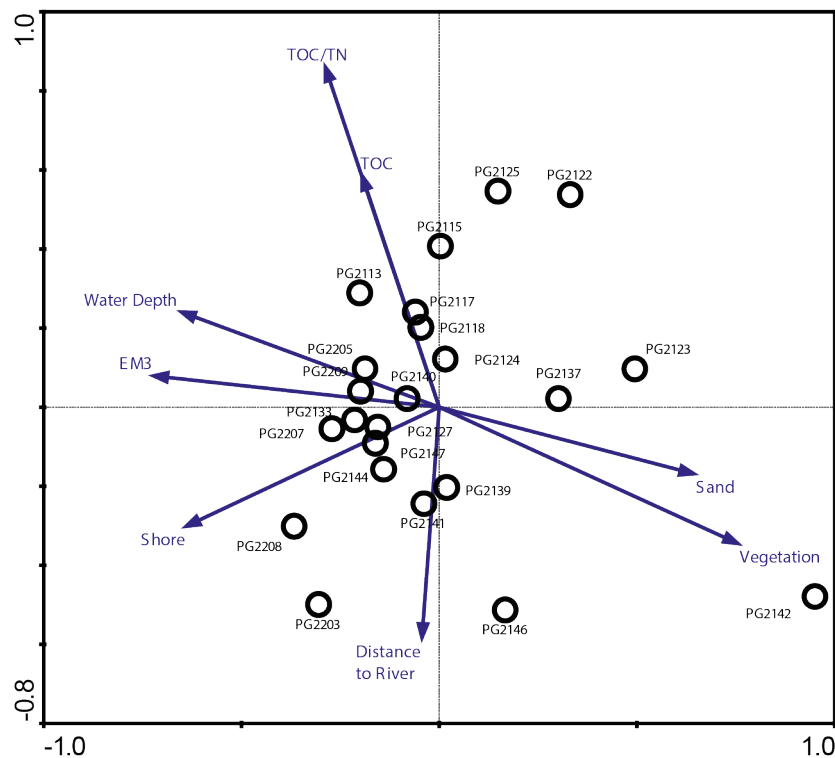
492 To guarantee the sustained availability of our research (Elger et al., 2016), the data
493 will be uploaded and freely accessible in the PANGAEA repository.

494

a. RDA, diatom species scores



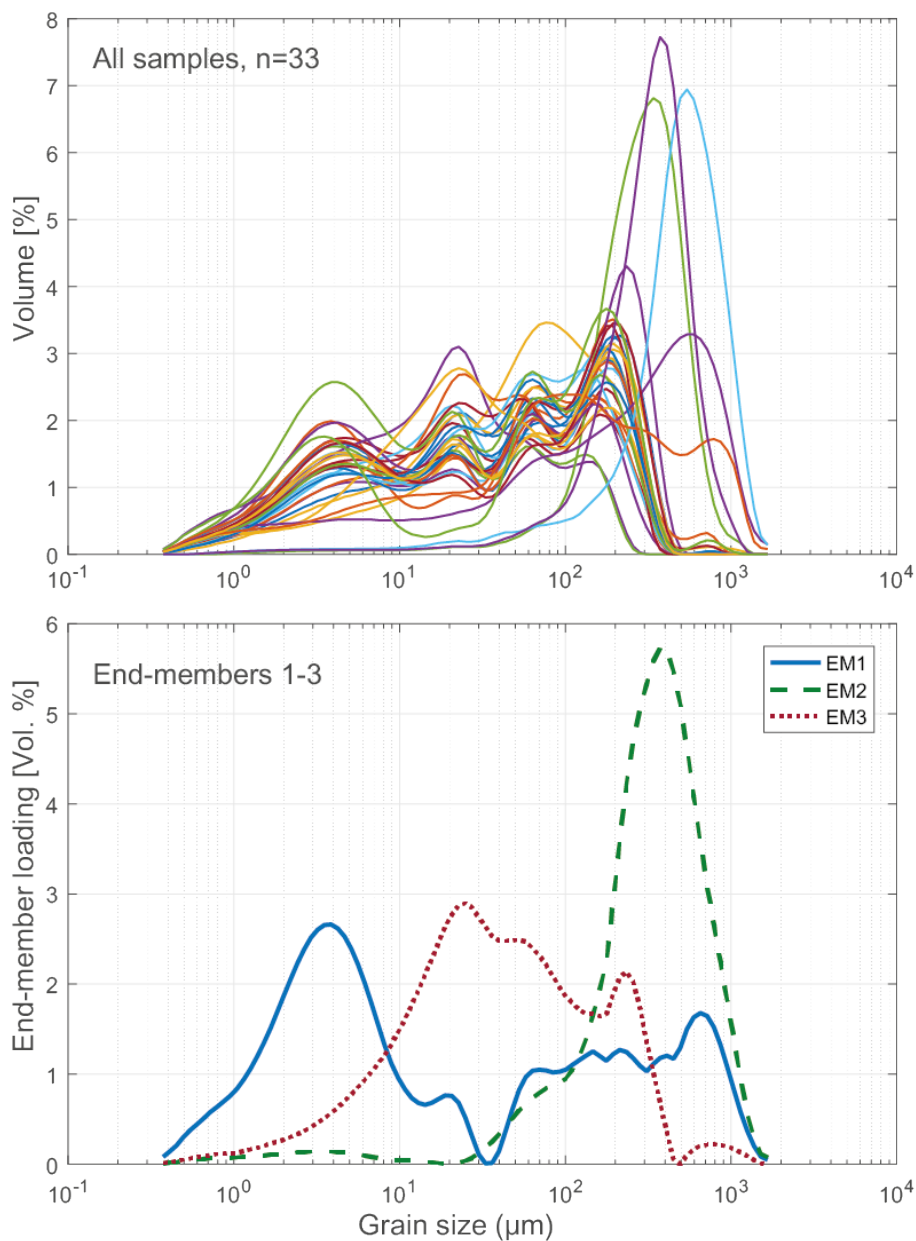
b. RDA, diatom samples scores



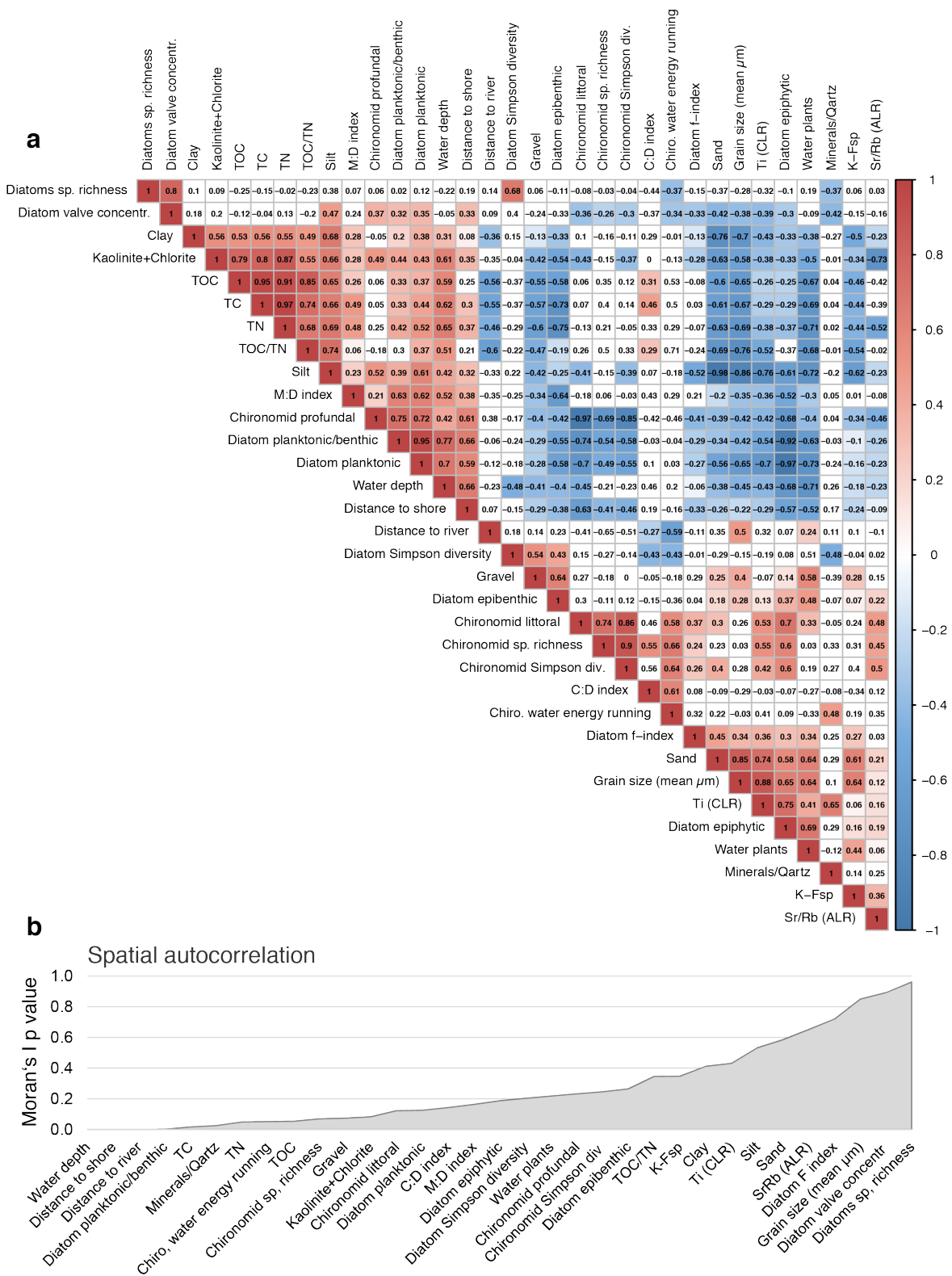
495
 496 **Fig. 2** RDA biplots of diatoms in the surface sediments of Lake Bolshoe Toko. (a) Common diatom taxa and
 497 significant environmental variables. (b) Diatom sampling sites and significant environmental variables. **Abbreviated**
 498 **species names:** AchBio - *Psammothidium bioretti*; AchDid - *Achnanthes cf. didyma*; AchHel - *Psammothidium*
 499 *helveticum*; AchLae - *Eucoconeis laevis*; AchLan - *Planothidium lanceolata*; AchLat - *Karayevia laterostrata*;
 500 AchLev - *Psammothidium levanderi*; AchOes - *Planothidium oestrupii*; AchSp - *Achnanthes sp.*; AchSub -

501 *Psammothidium subatomoides*; AchSuc - *Karayevia suchlandtii*; AmpPed - *Amphora pediculus*; AulAmb -
502 *Aulacoseira ambigua*; AulSub - *Aulacoseira subarctica*; AulVal - *Aulacoseira valida*; CocPla - *Cocconeis*
503 *placentula*; CycAto_ - *Cyclotella* cf. *atomus*; CycCom - *Cyclotella comensis*; CycCyc_ - *Cyclotella cyclopuncta*;
504 *Cyclri* - *Cyclotella iris*; CycSp - *Cyclotella comensis-tripartita-complex*; CymMin - *Encyonema minutum*; CymSin -
505 *Cymbella sinuata*; DiaMes_ - *Diatoma mesodon*; EncLun_ - *Encyonema lunatum*; FraCap - *Fragilaria capucina*;
506 *FraConVe* - *Stausira venter*; FraPin - *Fragilaria pinnata*; GomAcu - *Gomphonema acuminatum*; GomIns -
507 *Gomphonema insigne*; HipCos - *Hippodonta costulata*; NavCoc - *Cavinula cocconeiformis*; NavJae - *Cavinula*
508 *jaernefeltii*; NavPsc - *Cavinula pseudoscutiformis*; NitSp - *Nitzschia* sp.; PlioBol - *Pliocaenicus bolshetokoensis*;
509 *StaCon_* - *Stausira construens*.
510
511
512
513

521 HeteGri - *Heterotrissocladius grimshawi*-type; HetMaeo - *Heterotrissocladius maeaeri*-type 1; HetMaet -
 522 *Heterotrissocladius maeaeri*-type 2; HeteMar - *Heterotrissocladius marcidus*-type; Limnophy - *Limnophyes* -
 523 *Paralimnophyes*; MicroIn - *Micropsectra insignilobus*-type; MicrPed - *Microtendipes pedellus*-type; Orthocla -
 524 *Orthocladus/Cricotopus*; OrthOli - *Orthocladus oliveri*-type; OrthoS - *Orthocladus* type S; Paraclop -
 525 *Paracladopelma*; Paracri - *Paracricotopus*; ParaBat - *Parakiefferiella bathophila*-type; ParaTri - *Parakiefferiella*
 526 *triquetra*-type; Procladi - *Procladius*; Prodiam - *Prodiamesa*; Propsil - *Prosilocerus* type N; Protanyp - *Protanypus*;
 527 *Psectro* - *Psectrocladius* narrow; Pseudoch - *Pseudochironomus*; SergCor - *Sergentia coracina*-type; Smittia -
 528 *Smittia* - *Parasmittia*; Zavrelia - *Stempellinella* - *Zavrelia*; Synortho - *Synorthocladus*; TanyMen - *Tanytarsus*
 529 *mendax*-type; Tanytar - *Tanytarsus pallidicornis*-type 2; Tveteni - *Tvetenia bavarica*-type; ZaluMuc - *Zalutschia*
 530 *mucronata*-type; Chirono - Chironomini unidentified; Unid Tan - Tanytarsini unidentified; Unid Pen - Tanypodinae
 531 unidentified.
 532



533
 534 **Fig. 4** Endmember analysis grain-size distributions in 33 samples from Lake Bolshoe Toko.
 535
 536



538
539
540
541
542

Fig. 5 Correlation matrix of selected environmental parameters. a. Pearson correlation. Positive correlations indicated in red, negative correlations indicated in blue. To keep false discovery rate below 5%, only p values of <0.001 were used to assign colours (Colquhoun, 2014). b. Spatial autocorrelation associated to coordinates of sample sites. Shown as p values generated by Moran's Autocorrelation Coefficient (R package "ape").

544 4 Results

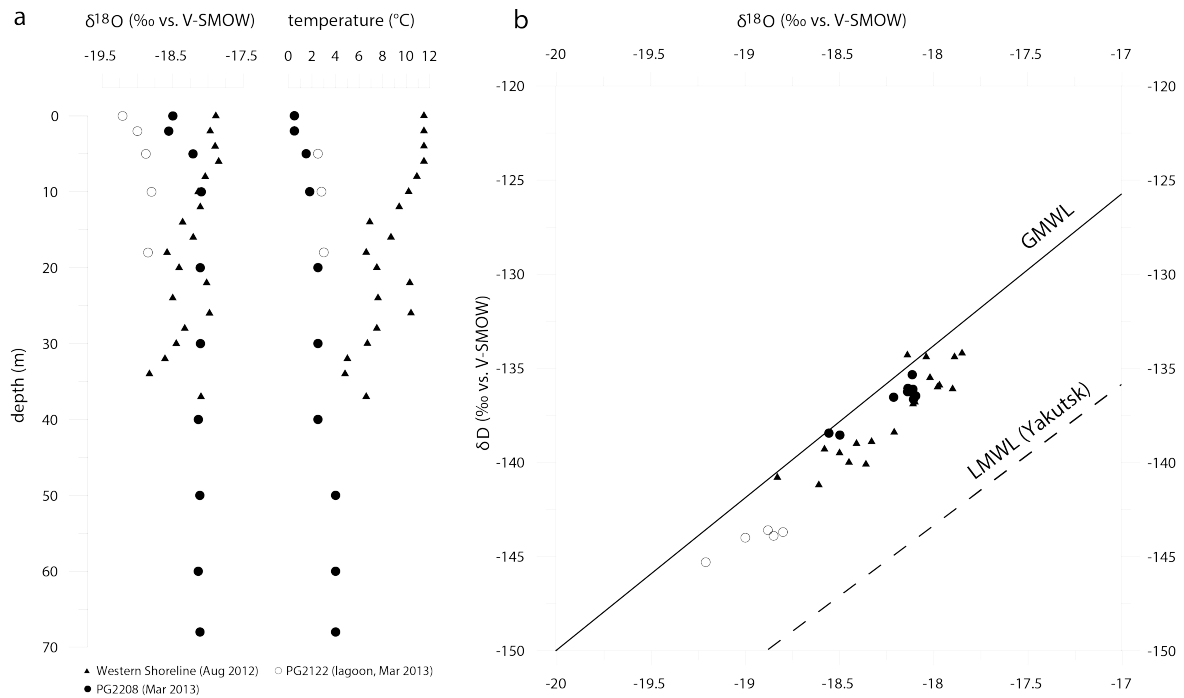
545 4.1 Water chemistry

546 Sampled surface waters of Bolshoe Toko (Table 1, ESM) were well saturated in O₂
547 (101-113 %) with a pH-values in the neutral range (6.8 – 7.2). Electrical conductivity
548 was very low for all waters (35.1–39.1 μS/cm), with slightly higher levels in the lagoon
549 (67.8 μS/cm). Traces of Al (mean 72 μg/L), Fe (mean 46.6 μg/L), and Sr (mean 37.1
550 μg/L) were present but there is no evidence of Pb, Cr, V, Co, Ni, Cu. Mean sulfate
551 concentrations (SO₄²⁻) was 2.35 mg/l on average, with lower values in the lagoon (0.51
552 mg/l). The concentrations of nitrate (NO₃⁻) was 0.76 mg/l, but lower in the lagoon (0.29
553 mg/l). HCO₃⁻ was 37.5 mg/l in the lagoon and 14.9 mg/l on average in the remaining
554 samples. There was no phosphorus in any sample. Overall the water can be
555 characterized as water of the Ca-Mg-HCO₃⁻ type.

556 Surface waters were characterized by mean isotope values of –18.7‰, –140.2‰
557 and 9.5‰ for δ¹⁸O, δD and d-excess, respectively (n=6). The isotopic composition
558 was relatively uniform in the main lake basin (δ¹⁸O = –18.58±0.15‰, δD = –
559 139±0.7‰), while the lagoon (PG2122) exhibited slightly lower δ¹⁸O (δD) values of –
560 19.2‰ (–145‰) (Fig. 6).

561 In March 2013 isotope-depth profiles at PG2208 exhibited a slight isotopic
562 enrichment trend from the surface to ~5 m-depth (~+0.35 ‰ for δ¹⁸O), with a relatively
563 uniform isotopic composition (δ¹⁸O = –18.2 ± 0.2 ‰) below 10 m (Fig. 6a). These
564 subtle variations likely reflect minor isotopic fractionation of surface waters during ice
565 formation in spring, and a well-mixed water column below. Conversely, the August
566 2012 depth profile at the Western Shoreline exhibited a gradual depleting isotope
567 trend below ~6 m depth, with marked variability that closely tracks water temperature
568 changes (Fig. 6a). Meteorological data from the nearby weather station (Toko RS, 10
569 km northward) recorded heavy rainfall for August 2012 (25 mm above the long term
570 mean of 83 mm). Such precipitation events could cause temporary isotopic
571 stratification or a variation in the isotopic signal throughout the water column. Due to
572 ongoing mixing, these variations were then evened. In conclusion, variations in the
573 isotopic composition throughout the August profile rather represent a temporal
574 phenomenon and not characteristic for Bolshoe Toko. In contrast, the lagoon showed
575 a lighter isotope composition (δ¹⁸O = –18.9 ± 0.2 ‰) than the main lake basin. All
576 samples were positioned close to the Global Meteoric Water Line (GMWL, Fig. 6)
577 indicating negligible evaporative effects on lake water isotope composition, and a
578 dominant influence of meteoric inputs both directly (i.e., precipitation) and indirectly
579 (i.e., river inflows). The Local Meteoric Water Line for Yakutsk (dashed line; δD = 7.59
580 * δ¹⁸O – 6.8), based on own data (monthly mean precipitation values between 1997

581 and 2006; n=106; from Kloss (2008), is given for comparison, and indicative for more
 582 continental climate conditions.



583
 584
 585
 586
 587
 588
 589
 590

Fig. 6: Hydrochemical situation between 2012 and 2013 in lake Bolshoe Toko. a. Profiles of water isotopes ($\delta^{18}\text{O}$) and temperature from different locations taken in August 2012 and March 2013. b. $\delta^{18}\text{O}/\delta\text{D}$ diagram for Bolshoe Toko lake water samples. GMWL is the Global Meteoric Water Line (black line), LMWL is the Local Meteoric Water Line for Yakutsk (dashed line; $\delta\text{D} = 7.59 * \delta^{18}\text{O} - 6.8$) based on own data (monthly mean precipitation values between 1997 and 2006; n=106; Kloss (2008)).

591 4.2 Physicochemical sediment composition

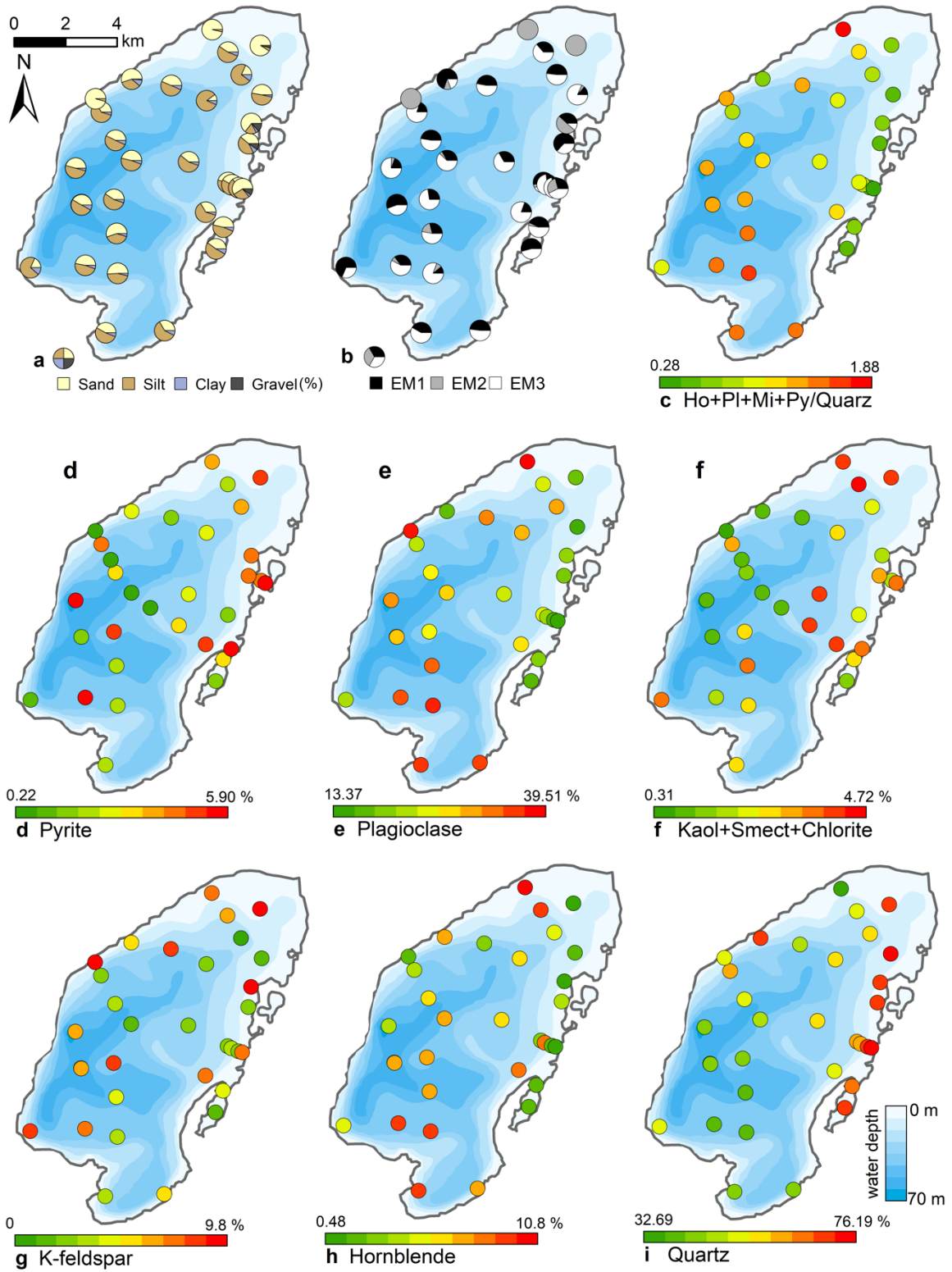
592 The typical surficial lake bottom sediments consisted of either brown organic-
 593 enriched gyttja or sandy, organic-poor siliciclastic material. Sand contents ranged
 594 between 10.2 % and 96.2 % (mean 45.9 %, Fig. 7); silt contents ranged from 3.6 %
 595 to 83.3 % (mean 47.1 %); clay contents ranged from 0.2 % to 11.3 % (mean 5.8 %).
 596 Gravel was found only in four samples at the north eastern near-shore areas with
 597 contents of up to 13.1 %. The mean grain size ranged from 12 to 479 μm (mean 72
 598 μm). The mean grain size generally correlated negatively with water depth (r -0.45).
 599 Mineral grains are composed mainly of quartz (32.7-76.2 %, mean 55.4 %),
 600 plagioclase (13.4-39.5 %, mean 26.2 %), K-feldspar (0.0-9.8 %, mean 5.6 %), and, to
 601 a smaller degree of pyrite (0.2-5.5 %, mean 3.3 %), hornblende (0.5-10.8 %, mean
 602 3.1 %), mica (0.3-2.4 %, mean 1.1 %), and the clay minerals smectite, kaolinite and
 603 chlorite (together 0.0-4.6 %, mean 2.0 %). The spatial distribution of minerals (Fig. 7)
 604 revealed a generally decreasing gradient of minerals relative to quartz starting from
 605 the Utuk river delta (proximal) towards the northern areas (distal).

606 The CLR transformed XRF data (Fig. 8) revealed high proportions of Zr and
607 intermediate to high Ti near the Utuk river inflow and at the northern and eastern
608 shore proximal areas. Zr values decreased with increasing water depth towards the
609 lake centre with the exception of the shallow lagoon, where low values were observed.
610 Mn values were highest in the lake centre and at the very deep site at the western
611 steep subaquatic slope, and intermediate at shallow areas close to the shore. A
612 minimum in Mn was found in the lagoon. Fe tends to be highest in the southern part
613 of the lake basin, in the very shallow site in the north, and in the lagoon. Br showed a
614 variable distribution; however, high values were found at 2 sites within the eastern
615 lagoon and correspond to high TOC contents.

616 Additive log ratios (ALR) of Mn/Fe were variable with intermediate values found at
617 sites surrounding the Utuk river inflow and low values within the lagoon and at basin
618 central sites. High values were located at the deepest lake site as well as in the
619 shallow north eastern region. Both Sr/Rb and Zr/Rb ratios showed high values directly
620 in front of the Utuk river inflow, and decreased with distance toward the basin center.
621 Both Sr/Rb and Zr/Rb exhibited intermediate to high values in the north eastern lake
622 region and lower values in the lagoon. Si/Ti ratio values demonstrated an increasing
623 trend from the southern lake region and lagoon to the northern lake region.

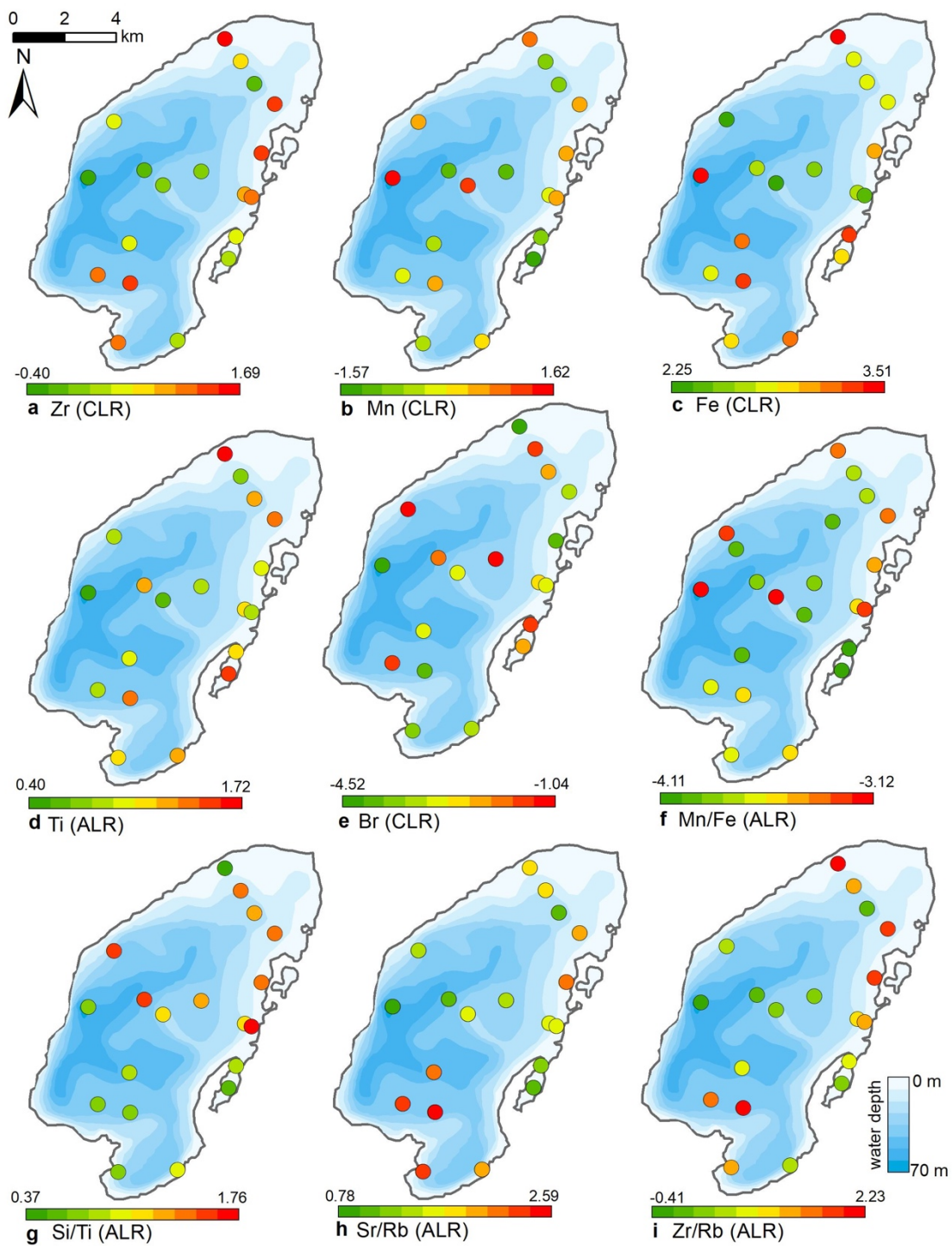
624 The contents of total organic carbon (TOC, Fig. 9) range from 0.1 % to 12.3 %
625 (mean 4.9 %). Maximum values occurred in the eastern area, intermediate values in
626 the central basin, and lowest in the northern shallow water areas. The difference
627 between TOC and total carbon is within the error of the devices and hence no
628 inorganic carbon was detected. TOC contents and the TOC/TN ratios were highest
629 near the Utuk river inflow in the southern part of the lake, in the lagoon, and in
630 proximity to the eastern shoreline. $\delta^{13}\text{C}$ was measured in 15 samples and showed
631 maximum values at the eastern shore (-25.7 ‰) and minimum values elsewhere (-
632 27.8 ‰).

633 Radiocarbon dating of surface sample at site PG2139 (0-0.5 cm) indicated an age
634 of 720 ± 30 ^{14}C yrs BP (Lab-ID: Poz-105350, NaOH-SOL), while PG2207 (0-0.5 cm)
635 suggested 1790 ± 130 ^{14}C yrs BP (Lab-ID: Poz-105355, NaOH-SOL. Considering that
636 the carbon concentration dissolved in sample PG2207 was too low (0.03 mgC), we
637 use sample PG2139 as an estimated reservoir effect to the lake caused by the input
638 of old carbon. Given that a hypothetical sediment surface is just a momentum only
639 collectable as a range of past surfaces and there was more time available for
640 radioactive decay at 0.5 cm depth than at 0 cm, the actual reservoir effect will be a
641 little bit lower and should be confirmed by ^{210}Pb and ^{137}Cs measurements of downcore
642 material before establishing an age depth model for sediment cores.



643
 644
 645
 646

Fig. 7 Spatial distribution of the grain-size and mineral compositions of the surface sediments of Lake Bolshoe Toko. Maps compiled in ArcGIS 10.4. Scales chosen as 10 classes with equal intervals.



647
648
649
650

Fig. 8 Spatial distribution of elements obtained from XRF measurements of surface sediments of Lake Bolshoe Toko. Maps compiled in ArcGIS 10.4. Scales chosen as 10 classes with equal intervals.

651 4.3 Diatoms

652 The Bolshoe Toko diatom assemblages were characterized by boreal and arcto-
653 alpine types, and exhibited distinct spatial variations across the lake. In total, 142
654 different diatom taxa were found at 23 sites, dominated by planktonic species
655 *Pliocaenicus bolshetokoensis* (Genkal et al., 2018) (0.0-27.9 %, mean 14.7 %),
656 *Cyclotella comensis* (0.0-23.1 %, mean 10.9 %), and benthic species *Achnantheidium*
657 *minutissimum* (0.0-38.0 %, mean 11.8 %). The relative content of planktonic species
658 (Fig. 9) was 2.0-73.7 % (mean 54.2 %), epiphytic species 19.2-83.9 % (mean 36.4
659 %), and epibenthic species 2.6-23.0 % (mean 9.3 %). The spatial distribution of the
660 main taxa are presented in Fig. 10. Small benthic fragilarioid species were
661 represented by 0.0-27.6 % (mean 7.4 %), Naviculoid species ranged from 3.3 % to
662 12.9 % (mean 7.2 %), and *Aulacoseira* species ranged from 0.0 % to 10.8 % (mean
663 4.5 %). *Pliocaenicus bolshetokoensis* maximum abundance occurred in areas of
664 deepest water such as the southern part of the lake and in the eastern lagoon.
665 *Cyclotella* species were more abundant in the central lake and were not as strictly
666 bound to water depth as *Pliocaenicus*. *Aulacoseira* species displayed no clear spatial
667 pattern, though were less abundant in the northern shallow water areas. *Tabellaria*
668 species were more abundant in shallow near-shore areas than in central and deep-
669 water areas.

670 Achnantheid (monoraphid) species were most abundant in near-shore areas,
671 especially near the eastern lake terrace. Fragilarioid (araphid) species were common
672 in the southernmost part near the inflow, as well as the lagoon. Other benthic species,
673 i.e. *Navicula*, *Cymbella*, and *Eunotia* were generally more abundant in shallow near-
674 shore areas than in deeper water areas.

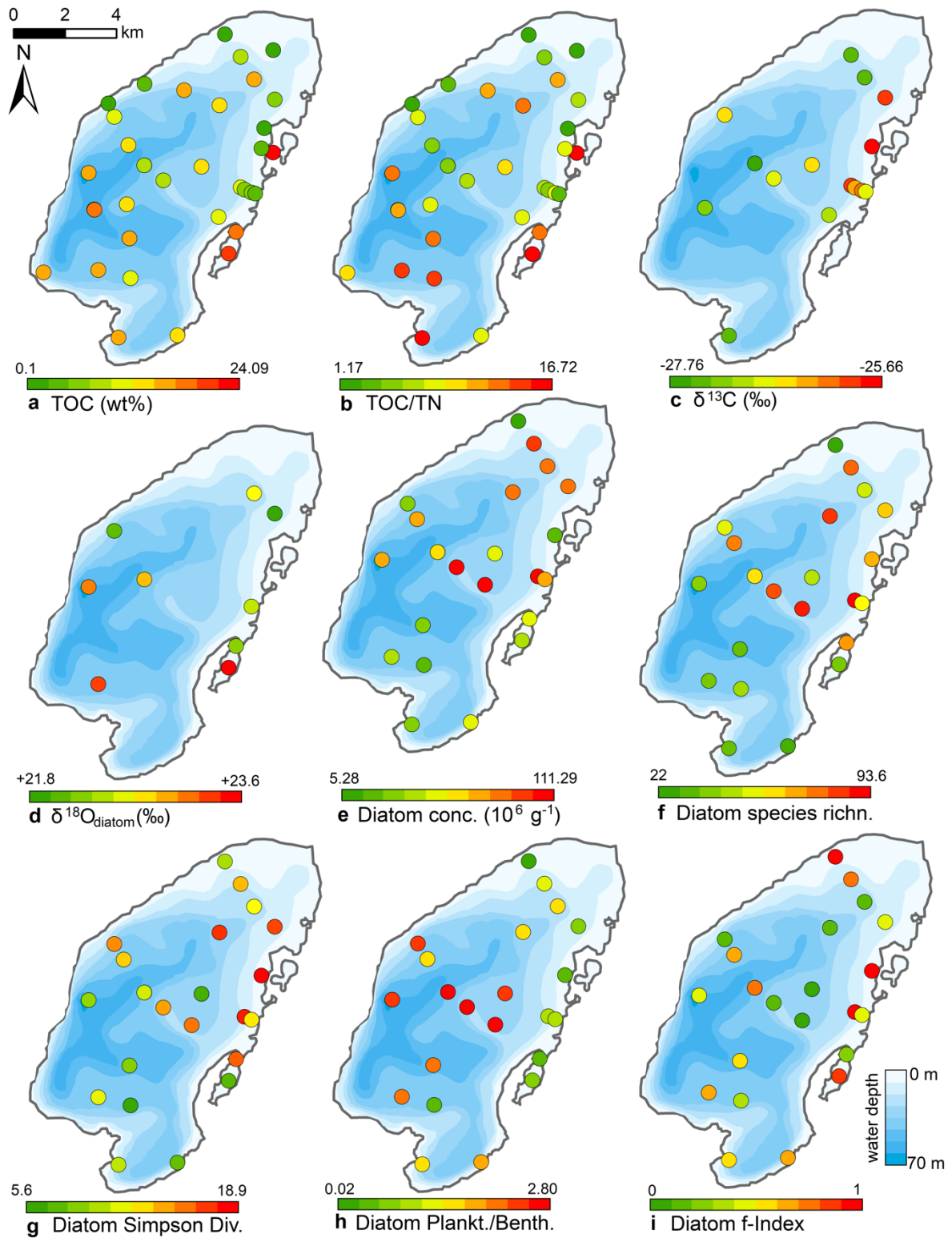
675 In pelagic areas planktonic diatoms were generally more abundant than epiphytic
676 and epibenthic species. Epiphytic species, however, predominated in some shallow
677 areas in the north and east parts of the lake. Epibenthic species occurred in smaller
678 abundancies in shallow lake littorals. Together with an increased amount of non-
679 planktonic species, the Simpson diatom species diversity was higher in northern and
680 eastern parts of the lake. The chrysophyte index was high near the river inflow in the
681 south and along the river-like bathymetrical structure, as well as the lagoon where
682 another small river inflowed into the lake. The *Mallomonas* index, reported for high
683 nutrients and low pH (Smol et al., 1984), was highest near the inflow and in the central
684 part, and lowest at near-shore areas in the north and east. The maximum f-index
685 value, representing the highest valve preservation, was found in the near shore areas,
686 whereas lower values were found at the shallow bathymetrical structure in the central
687 part of the lake. Maximum valve concentrations were observed in the central and
688 northern lake basin.

689 The initial RDA with all environmental variables indicated that axes 1 and 2
690 explain 39.6 % of variance in diatom species data. After deleting all intercorrelated

691 variables, 13 parameters with VIFs <20 were left for manual selection with Monte-
692 Carlo test. The analysis revealed 8 statistically significant ($p \leq 0.05$) explanatory
693 variables: TOC/TN, TOC, water depth, distance from River, distance from the shore,
694 presence of vegetation, sand, and EM3, (ESM diatoms, Fig. 2). Eigenvalues for RDA
695 axes 1 and 2 constrained by eight significant environmental variables constitute 81%
696 and 59%, respectively, of the initial RDA, suggesting that the selected significant
697 variables explain the major variance in the diatoms data. The RDA biplots of the
698 species scores and sample scores (Fig. 2) show that diatom species and sites are
699 grouped according to the main environmental forcing responsible for their spatial
700 distribution. The clearest environmental signals in the RDA are related to water depth,
701 habitat preferences and river influence. The upper left quarter of the biplot is strongly
702 influenced by water depth, grain size (EM3), and the ratio between TOC and TN. The
703 species found next to water depth are planktonic *Cyclotella* taxa, whereas *Aulacoseira*
704 is closer to TOC/TN and the total carbon content. In the lower right quarter epiphytic
705 and benthic taxa prevail, i.e. achnanthoid, naviculoid and cymbelloid taxa, associated
706 to the presence of vegetation and coarser (sand) substrate conditions. The distances
707 to river and to shore are crossing the lower left quarter and are associated to different
708 planktonic *Cyclotella* and achnanthoid taxa, while in the opposite direction, with
709 increasing Utuk river influence, fragilarioid taxa, *Eunotia*, *Tabellaria*, and
710 *Gomophonema* prevail, next to the high influence of TOC/TN.

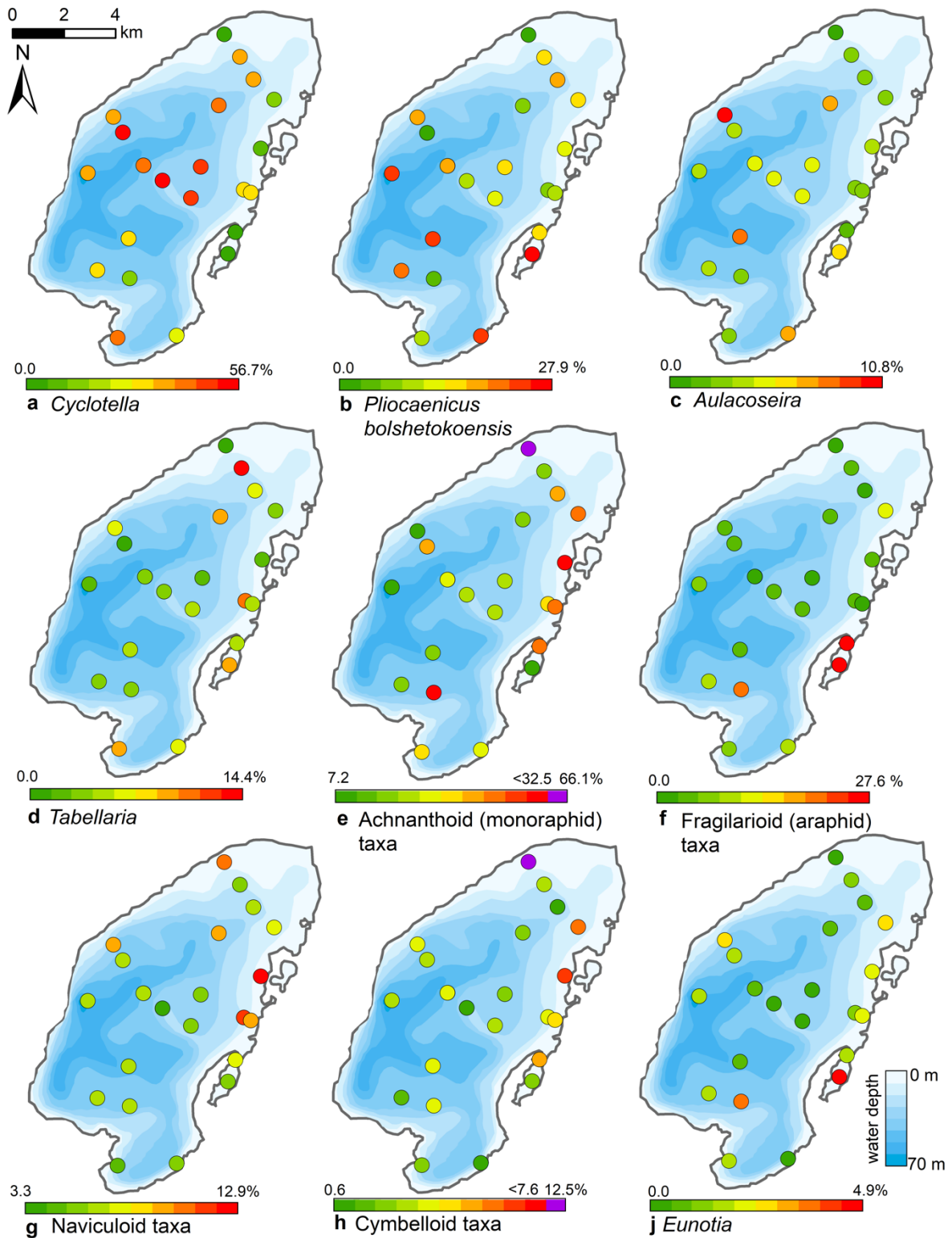
711 Mean surface sediment $\delta^{18}\text{O}_{\text{diatom}}$ was 22.8 ‰ (min. 21.9 ‰, max. 23.6 ‰, $n=9$,
712 Fig. 9) with a standard deviation of ± 0.6 ‰ (1σ). The spatial distribution indicated
713 higher values ~ 23.3 ‰ in the deeper south-western part of lake (PG2113, 2115, 2005)
714 and lower values ~ 22.3 ‰ in the shallower northern lake basin (PG2139, 2140, 2147,
715 2209). The two samples from the lagoon exhibited values of 22.2 ‰ in the shallower
716 northern area and 23.6 ‰ in the deeper part. Four samples from the southern part
717 could not be purified well enough and had contamination corrections >2 ‰.

718



719
720
721
722
723

Fig. 9 Spatial distribution of organic properties and statistical parameters inferred from diatom assemblages in the surface sediments of Lake Bolshoe Toko. Maps compiled in ArcGIS 10.4. Scales chosen as 10 classes with equal intervals.



724
725
726
727
728
729

Fig. 10 Spatial distribution of main diatom taxa in the surface sediments of Lake Bolshoe Toko. Maps compiled in ArcGIS 10.4. Scales chosen as 10 classes with equal intervals. Maps e and h had exceptionally high values of achnantheid and cymbelloid taxa only in the very shallow (0.5 m) site PG2142. These values are shown in purple, indicated separately at the right side of the scales.

730 4.4 Chironomids

731 A total 79 different chironomid taxa were present in the surface sediment samples,
732 of which 48 belong to the subfamily Orthocladiinae, 25 to Chironominae (15 from the
733 triba Tanitarsini and 10 from the triba Chironomini), four taxa were from subfamily
734 Diamesinae, and 2 from Tanypodinae.

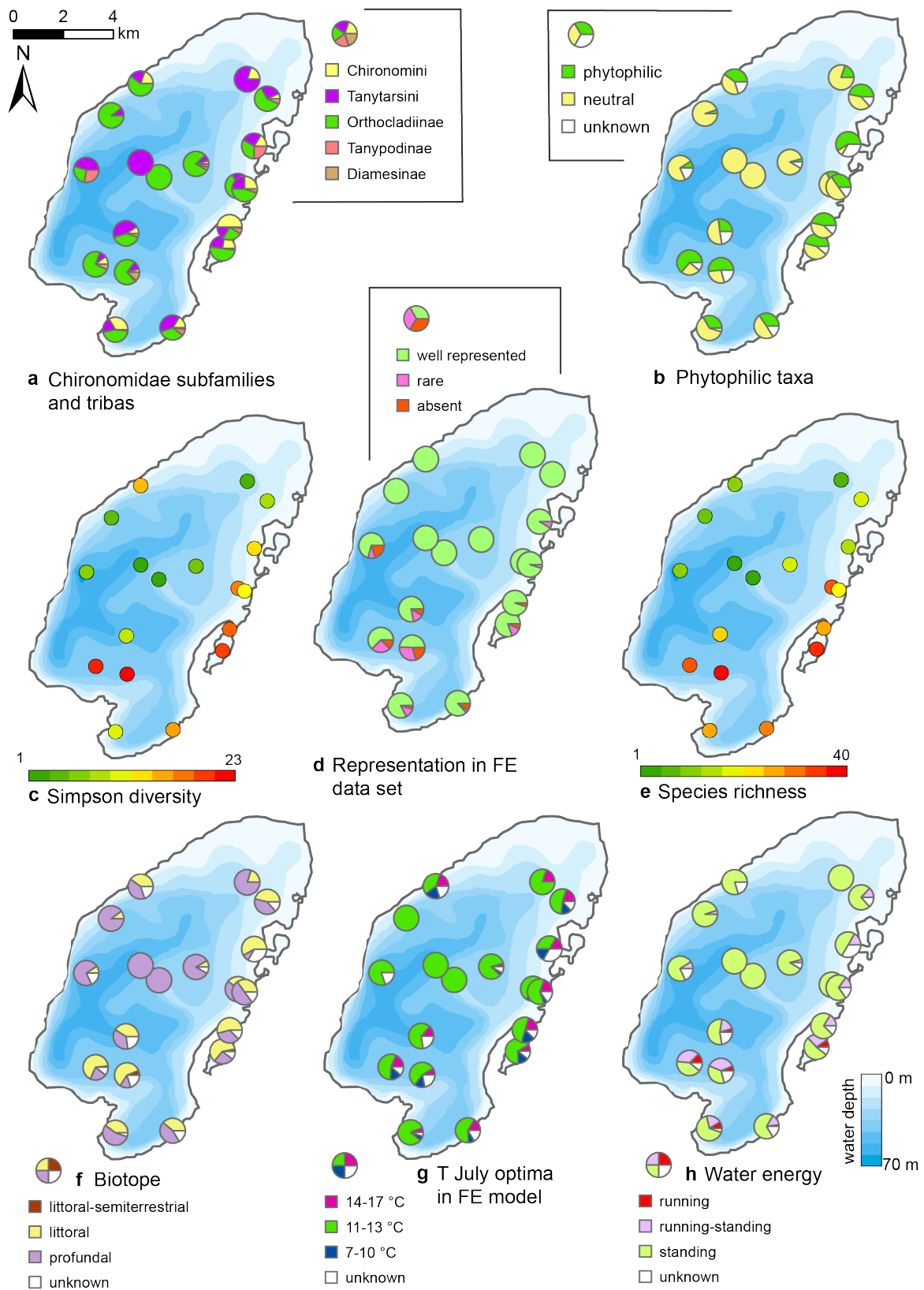
735 The initial RDA with all environmental variables shows that axes 1 and 2 explain
736 46.7% of variance in the taxon data. Most of the environmental parameters were
737 intercorrelated, and following sequential deletion of all redundant variables, eight
738 parameters with VIFs <20 remained for the further analysis. The manual Monte-Carlo
739 test selection demonstrates four statistically significant ($p \leq 0.05$) explanatory
740 variables: TOC/N, water depth (WD), distance from River, and presence of vegetation
741 (Table 2). Distance from the river and presence of vegetation showed lower than
742 TOC/N and WD level of significance. However, we still use these parameters for
743 interpretation of the chironomid data as there was a clear gap between the 4 chosen
744 parameters ($p = 0.001$ to 0.059) and much higher p values (>0.25) of the following
745 tested parameters (TC, distance to the shore, silt, clay). Eigenvalues for RDA axes 1
746 and 2 constrained by four significant environmental variables were 0.200 and 0.150,
747 respectively, and constituted 70 and 85 % of the RDA performed on all environmental
748 variables (0.289 and 0.177, respectively). This minor difference suggests that the four
749 selected variables sufficiently explain the major gradients in the chironomid data.

750 The RDA biplot of the sample scores shows that sites are grouped by their
751 location in relation to the major environmental variables (Fig. 11), and distribution of
752 chironomid taxa along the RDA axes reflects their ecological spectra. Fig. 11 and
753 Table 6 in the ESM show median values of eco-taxonomical chironomid groups and
754 their relation to environmental parameters.

755 Sites most strongly influenced by the inflowing rivers grouped in the lower left
756 quadrant of the biplot, as the vector in the upper right quarter shows increasing
757 distance from the river mouth. In total 64 chironomid taxa were found in this group of
758 sites, and of these 33 were only found here. Chironomid fauna were chiefly
759 represented by phytophilic littoral taxa from the Orthocladiinae genera *Cricotopus*,
760 *Orthocladus*, *Eukiefferiella*, and *Parakiefferiella* etc. (Fig. 11). Another important
761 feature is the presence of a relatively high amount of lotic environmental taxa, among
762 which are several *Diamesa* taxa, *Rheocricotopus effusus*-type, *Synorthocladus*,
763 *Brillia*, and for lotic-lentic environments *Parakiefferiella bathophila*-type, *P. trigueta*-
764 type, *Nanocladus rectinervis*-type, *N. branchicolus*-type, several *Eukiefferiella* taxa,
765 and *Stictochironomus*.

766 The group in the opposite upper right quadrant represents the northern part of
767 the lake situated far from the inflowing rivers. Here, mainly profundal taxa prevail, i.e.
768 *Procladius*, *Polypedilum nubeculosum*-type, *Cryptochironomus* (eurytopic), and
769 *Heterotrissocladus maeaeri*-type 1 (acidophilic).

770 The lower right group of sites represent eastern shallow littoral with presence of
771 macrophytes. Species richness and proportion of semiterrestrial and littoral taxa in
772 this group is generally low. Littoral taxa were generally phytophilic: *Cricotopus*
773 *intersectus*-type, *C. cylindraceus*-type, *Dicrotendipes nervosus*-type (mesotrophic),
774 and *Cladotanytarsus mancus*-type and *Psectrocladius sordidellus*-type (acid-tolerant
775 mesotrophic). Most abundant profundal taxa here belong to the acid-tolerant
776 *Heterotrissocladius* genera represented by *H. macridus*-type, *H. maeaeri*-type 1 and
777 2, *H. grimschawi*-type (acidophilic), and to the subfamily Tanypodinae represented by
778 *Procladius*. The sites grouped in the opposing upper left quadrant represent lotic and
779 lotic-lentic taxa (*Diamesinae*, *Thenimaniella clavicornis*-type, *Eukiefferiella*
780 *claripennis*-type, *Eukiefferiella fittkaui*-type, several *Orthocladius* taxa).
781



782
783
784
785

Fig. 11 Spatial distribution of chironomid taxa and inferred statistical parameters in the surface sediments of Lake Bolshoe Toko. Maps compiled in ArcGIS 10.4. Scales chosen as 10 classes with equal intervals.

786 5 Discussion

787 5.1 Spatial control of abiotic and biogeochemical sediment components

788 Sediment-geochemical and physical properties of the uppermost surface of the
789 sediment basin in Bolshoe Toko are spatially variable. Physical properties of particles
790 within the surface sediments depend chiefly on transportation processes and the
791 characteristics and availability of clastic compounds in the lake catchment. The main
792 catchment comprises the Stanovoy mountain range in the south channelled through
793 the Utuk river into Bolshoe Toko. Accordingly, the lake experiences annual input of
794 suspended material through a single source at the Utuk river mouth that likely is at its
795 maximum during spring snow melt (Bouchard et al., 2013). The grain-size data and
796 its end-members (Fig. 4 and 7) indicate that the relative proportions of sand, silt, and
797 clay are somewhat constant in proximity to the Utuk river inflow but change towards
798 the north and at the lake shoreline. Whereas in the central northern lake basin the
799 amount of silt increases, the proportions of sand increase along the northern shoreline
800 on top of the drowned moraine. Gravel is only present in samples near the lake
801 terraces in the east. The constant distribution in the south-central lake basin reflects
802 the river input. Decreasing river influence and hence decreasing water transport
803 energy with increasing distance from the river mouth leads to the observed
804 predominance of finer grain-sizes (silt dominated) samples in the northern central
805 parts of the lake. Sandy samples along the shoreline reflect direct input from the
806 moraines around the northern part of the lake. Other relevant within-lake sedimentary
807 processes include shore-erosion and inwash and winnowing of fine sediment grains
808 by surface currents as well as alluvial processes and debris flows which continue
809 basin ward as subaquatic flows. The restriction of gravel at the eastern shore can be
810 attributed to the availability of source material and suitable transport pathways of
811 coarser clasts from the third moraine. In consequence to the described lateral
812 transport trajectories and local control factors within the lake, there is only weak
813 negative correlation between mean grain size and water depth ($r -0.45$, Fig. 7 and
814 12).

815 The modelled end-member loadings of the observed grain-size classes (Fig. 4 and 7)
816 indicate an EM1 major peak in fine silt that represents fluvial sediment input. EM2 has
817 peak values in fine to medium sandy grain-size fractions and in the northern part of
818 the lake indicative of depositional processes associated with the erosion of moraines
819 distal from the river inflow, where the hydrological dynamics in the lake basin are
820 weak. The weak positive correlation between EM3 and the concentration of diatom
821 valves ($r 0.44$) likely represents both *in-situ* diatom valves that could not be removed
822 from allochthonous sediment particles during sample processing, and possibly
823 redistributed ice-rafted debris (Wang et al., 2015).

824 Intermediate concentrations of TOC and high ratios of TOC/TN in the south as
825 compared to the north suggest differences in catchment characteristics, i.e. a
826 considerable allochthonous contribution of terrestrial plant material from the Utuk
827 river. This assumption is supported by previous findings that show non-vascular
828 plants, i.e. phytoplankton and other algae, with TOC/TN ratios between ca. 5 and 10
829 while organic matter from vascular land plants has higher values of about 20 (Meyers
830 and Teranes, 2002). High values of TOC/TN in lake sediment surfaces at river inflows
831 have also been observed in other studies (Vogel et al., 2010). $\delta^{13}\text{C}$ is generally low
832 on average (-26.8‰) and only slightly higher at the eastern shore (-25.7‰),
833 suggesting a strong overall dominance of C_3 plants and phytoplankton in the bulk
834 organic matter fraction (Meyers, 2003). It remains unclear as to the degree of old and
835 reworked organic carbon, e.g. from charcoal deposits, transported to the lake.

836 The distribution of elements from the XRF scanning data suggests strong abiotic
837 relationships to grain-size and mineral distributions. We focus on heavier elements
838 because lighter elements, even though commonly in higher concentrations, show
839 potential contribution from multiple sources. Sr/Rb ratios and Zr are negatively
840 correlated with Kaolinite/Chlorite (r -0.73 and -0.85, respectively). As described in
841 Kalugin et al. (2007), Rb substitutes for K in clay minerals. The Sr/Rb ratios do not
842 however show a significant correlation with grain-size parameters, as found in other
843 studies (Biskaborn et al., 2013b). We assume therefore that Sr, as substituent for Ca,
844 is influenced by multiple minerals represented in different grain-size fractions, i.e. K-
845 feldspar (r 0.45) and Hornblende (r 0.24). Associated to high metamorphic grades in
846 the Stanovoy mountains, Sr is preferentially taken into the K-feldspar phase (Virgo,
847 1968). Conversely, the Zr/Rb ratio correlates well with the sand fraction (r 0.50) and
848 with the mean grain size (r 0.49), but negatively with silt (r -0.54) and clay (r -0.39).
849 We account for this effect by a higher diversity of minerals in the input of the Utuk
850 river supplying the lake basin with mafic Ca-rich metamorphic rocks from the
851 Stanovoy mountains. The strong influence of the Utuk river in the spatial distribution
852 of physicochemical sediment components is further demonstrated by the decreasing
853 gradient of minerals relative to quartz starting from the Utuk river towards the northern
854 lake basin (Fig. 7). The most representative indicator of grain size variations in surface
855 sediments is given by clr transformed values of Ti, which correlate well with the sand
856 fraction (r 0.74) and the mean grain size (r 0.88).

857 Si/Ti ratios have traditionally been used as a proxy for the biogenic silica content
858 of sediments (Melles et al., 2012). This stems from the fact that Ti is generally
859 attributed to detrital influx and Si to both detrital and biogenic (diatom) origins. At
860 Bolshoe Toko positive correlations between Si/Ti ratios, diatom valve concentrations
861 (r 0.36) and the ratio of planktonic to benthic diatoms (r 0.42) suggests that Si/Ti may
862 be useful to trace the relative portion of diatom valves in intermediate grain-size
863 fractions. Moreover, the Si/Ti ratio correlates significantly with silt (r 0.81).

864 Mn/Fe ratios have been ascribed to redox dynamics associated to bottom water
865 oxygenation processes (Naeher et al., 2013). In Bolshoe Toko, however, the detrital
866 input of ferrous minerals, i.e. pyrite, suggests that Mn/Fe ratios cannot be directly
867 attributed to redox processes in the surface sediments. This is supported by the
868 correlation of Fe with the sand fraction (r 0.6) and grain-size (r 0.59). Accordingly, we
869 found no significant correlations between Mn/Fe and other abiotic or biotic proxies.

870 Lastly, there is an uncertainty in the spatial distribution of elements measured by
871 XRF techniques. We attribute this lack of clear patterns to: (1) methodological hurdles
872 to apply XRF techniques to surface sediments commonly rich in water and organic
873 material, and (2) multiple sources of the same elements coming from minerogenic
874 input, grain-size differences in individual samples and different intensities of redox
875 processes at different habitat settings. The high variance of elements are therefore
876 representative of the high complexity of this lake system, rather than unequivocal
877 validations or falsifications of the applicability of XRF scanner data as an
878 environmental proxy at Bolshoe Toko.

879
880

881 **5.2 Factors explaining the spatial diatom distribution**

882 Diatom communities in Yakutia respond rapidly to environmental changes
883 including hydrochemical parameters, water depth, nutrients, and catchment
884 vegetation type (Pestryakova et al., 2018). Planktonic diatom species are ubiquitous
885 across Bolshoe Toko, with a distinct tendency of the ratio between planktonic and
886 benthic species to greater water depths (r 0.77, Fig. 5 and 12), due to the limited
887 availability of light for benthic species (Gushulak et al., 2017; Raposeiro et al., 2018).
888 Especially *Aulacoseira* species were never abundant along the shallower northern
889 and eastern shorelines. The primary difference between the two most abundant
890 genera in the lake is that *Pliocaenicus* exhibits highest abundancies proximal to the
891 inflow and in the southeastern lagoon, whereas *Cyclotella* are more abundant in the
892 lake center and absent in the lagoon. Little is yet known about the new species
893 *Pliocaenicus bolshetokoensis* (Genkal et al., 2018). Our findings suggest factors other
894 than water depth (r 0.39), such as proximity (e.g. nutrient supply) to the Utuk river and
895 small streams, as controlling parameters for bloom intensities of this species.
896 *Cyclotella*, however, is restricted to stratification of the water column and hence more
897 abundant at distance from the river mouth, where incoming water causes turbulence
898 (Rühland et al., 2003; Smol et al., 2005). *Cyclotella* is therefore also believed to benefit
899 from recent air temperature warming trends and will likely increase in abundance
900 (Paul et al., 2010). *Aulacoseira* is a dense, rapidly-sinking tycho planktonic group of
901 species requiring water turbulence to remain in the photic zone (Rühland et al.,
902 2008; Rühland et al., 2015), which explains the lower abundancies in the northern and

903 hydrologically less dynamic zones within the lake. Lightly silicified *Tabellaria* species
904 are known to occur in zigzag planktonic colonies, yet, they also appear as short-
905 valved populations in the benthos (Lange-Bertalot et al., 2011; Biskaborn et al.,
906 2013a; Krammer and Lange-Bertalot, 1986-1991). In Bolshoe Toko, the spatial
907 distribution of *Tabellaria* indicates benthic habitats are more favourable than
908 planktonic.

909 The most common non-planktonic species in Bolshoe Toko belong to achnantheid
910 (monoraphid) genera, of which most species are epiphytic. Epiphytic species exhibit
911 a stronger negative correlation to water depth ($r = -0.68$) than epibenthic species ($r =$
912 0.4), indicating that aquatic plants, in turn controlled by water transparency, pH, water
913 depth and nutrient status (Valiranta et al., 2011), have an important function in the
914 lake ecosystem (Fig. 12). The highest abundance of achnantheid and cymbelloid
915 valves occurs at 400 m distance to the northern shore at a water depth of 0.5 m.

916 Fragilarioid species are adapted to rapidly changing environments and are thus
917 good indicators of ecosystem variability (Wischnewski et al., 2011). The peak
918 occurrences of *Staurosira* species, which are pioneering small benthic fragilarioids
919 (Biskaborn et al., 2012), therefore indicates the formation of a new ecosystem habitat
920 type in the lagoon at the south-eastern lake basin. We assume this basin is
921 successively separated from the main basin and will eventually form a small isolated
922 remnant lake, similar to "Banya" lake (Fig. 1). High productivity of epiphytic species
923 and low detrital input suggested by elemental and grain-size data, together with higher
924 organic content (High TOC and Br), indicate a calm sedimentological regime with high
925 bioproductivity. Similar neutral pH values measured in water samples from the central
926 basin and the lagoon (Table 1) questions pH as a main driving factor of the *Eunotia*
927 peak in the lagoon. However, Barinova et al. (2011) suggest 5.0-5.8 pH range for the
928 identified *Eunotia* species, which rather indicates that the pH values obtained during
929 April in 2013 are not representative for the annual average and the specific catchment
930 of the lagoon, which likely will differ from this point measurement. The ice break-up
931 during spring and transport of water from the catchment restricted to the lagoon likely
932 leads to milieu differences in the lagoon relative to the main basin.

933 High autocorrelation coefficients (Moran's I p values) for species richness and
934 valve concentration indicate strong local influence of biotic processes, i.e.
935 reproduction, leading to spatial autocorrelation (Legendre et al., 2005). The lowest
936 observed autocorrelation for the diatom planktonic/benthic ratio confirms the strong
937 relationship between diatom species assemblage composition and water depth. A
938 strong relationship between diatom diversity and water depth is supported by a study
939 comparing morphological count data and phylogenetic species data gained by next-
940 generation sequencing DNA analysis (Stoof-Leichsenring et al., in review).

941 The RDA biplot of diatoms (Fig. 2) suggests that both water depth and distance to
942 river are important lake attributes accounting for the species distributions across the

943 lake. Especially *Eunotia*, fragilarioids, *Tabellaria*, and also *Aulacoseira subarctica*
944 appear more frequently at sites that are close to the Utuk river mouth (e.g. PG2113,
945 PG2115, PG2117, PG2118). The high TOC/TN ratios in these samples illustrates the
946 strong riverine input of allochthonous material. In the biplots, high water depth is
947 primarily associated to *Cyclotella* species (and *Aulacoseria*), while *Aulacoseira*
948 species tend to be additionally influenced by incoming rivers and also thrive closer to
949 the shorelines. Areas close to river mouths are usually dominated by river taxa and
950 species that prefer higher nutrient content related to river input and associated early
951 ice cover melting (Kienel and Kumke, 2002). Accordingly, the influx of diatoms from
952 wetlands in the lake catchment is an important additional factor influencing the spatial
953 diatom distribution (Earle et al., 1988). Compared to direct conductivity, water depth
954 and nutrient controls, the link between temperature and diatom species is poorly
955 understood in Yakutian lake systems (Pestryakova et al., 2018) and should be
956 avoided.

957 Our RDA also shows that a high diversity of benthic, and particularly epiphytic
958 diatom species, i.e. several acnathoid species and some naviculoid taxa, plot in
959 the opposite direction from water depth together with vegetation and the coarse grain-
960 size fraction. Kingston et al. (1983) revealed spatial diatom variability in the Laurentian
961 Great Lakes, where the stability of diatom assemblages increased with water depth.
962 In shallower marginal waters of the Great Lakes, the availability of diverse habitats,
963 including benthic and periphytic niches, leads to high species diversity. According to
964 our data in Bolshoe Toko, the Simpson diversity index suggests higher effective
965 numbers of dominant species associated to increased habitat complexity (Kovalenko
966 et al., 2012), i.e. availability of water plants and benthic substrates in shallower depths
967 along the eastern and northern shore. Thus, higher diversity in this area is facilitated
968 by differential catchment preferences. However, it can be assumed that due to lesser
969 water supply rates from the small northern part of the catchment (Fig. 1), a single
970 location at the north eastern lake margin will likely not receive significantly higher
971 loadings of nutrients as compared to the Utuk river coming from the igneous mountain
972 range. Nevertheless, moraine deposits typically contain high amounts of silt and clay
973 which can more easily be weathered and altered to fertilizing substances that are
974 transported into the calm and shallower northern part of the basin.

975 The indices of chrysophyte cysts and *Mallomonas* relative to diatom cells exhibit
976 indistinct patterns in spatial distributions, but a slight tendency towards proximity to
977 river input and high water depths. Although chrysophyte cysts commonly represent
978 planktonic algae (Smol, 1988b), periphytic taxa are also common in boreal regions
979 (Douglas and Smol, 1995) with cool and oligotrophic conditions (Gavin et al., 2011).
980 *Mallomonas* was reported as an indicator of lake eutrophication and acidification
981 (Smol et al., 1984).

982 Taphonomic effects on the preservation of subfossil assemblages are generally
983 influenced by clastic transport mechanisms depending on the lake morphology
984 (Raposeiro et al., 2018). The preservation of diatom valves in Bolshoe Toko is found
985 to be lowest in samples from a plateau-like feature at the central part of the lake
986 bottom, which indicates increased re-working associated to bottom currents and/or
987 increased dissolution of diatom valves due to lesser accumulation rates, and/or
988 increased grazing activity of herbivorous organisms (Flower and Ryves, 2009; Ryves
989 et al., 2001).

990 The spatial distribution of $\delta^{18}\text{O}_{\text{diatom}}$ from the sediment surface indicates higher
991 $\delta^{18}\text{O}_{\text{diatom}}$ values at the deeper, south-western part of the lake with a difference of app.
992 1‰ compared to lower $\delta^{18}\text{O}_{\text{diatom}}$ values in the shallower northern part. This could
993 reflect a combination of spatial $\delta^{18}\text{O}_{\text{water}}$ variations, water temperatures, and/or a
994 potential species-driven fractionation effect. However, existing studies demonstrate
995 no apparent species composition effects on lacustrine $\delta^{18}\text{O}_{\text{diatom}}$ (Bailey et al.,
996 2014; Chaplignin et al., 2012b). Additionally, the sieving step reduces the assemblage
997 before the isotope analysis to a small size interval resulting in a similar species-
998 composition. Furthermore, dissolution effects in nature and during sample preparation
999 could have an impact on $\delta^{18}\text{O}_{\text{diatom}}$. However, we suppose differential dissolution to
1000 have minor influence on the spatial variability of $\delta^{18}\text{O}_{\text{diatom}}$ at BT samples tackled in
1001 our study as these are (1) of similar age, (2) have been treated with wet chemistry at
1002 low temperatures and (3) after preparation do not show any microscopical signs of
1003 dissolution effects, i.e. a low diatom dissolution index (Smith et al., 2016).

1004 Regarding $\delta^{18}\text{O}_{\text{water}}$ variability, waters sampled at the same time in different parts
1005 of the lake show a uniform isotopic composition (within $\pm 0.15\text{‰}$) and indicate an
1006 isotopically well-mixed lake. Considering this is a one-time recording, slight seasonal
1007 variation between shallower and deeper parts (for example due to evaporation)
1008 cannot be excluded and could account for some differences in ^{18}O . However, lake
1009 surface evaporation would result in isotopic enrichment and overall higher $\delta^{18}\text{O}_{\text{diatom}}$
1010 values.

1011 Alternatively, the lake temperature in which the diatoms grow has an impact of ca.
1012 $-0.2\text{‰}/^{\circ}\text{C}$ on $\delta^{18}\text{O}_{\text{diatom}}$ (Brandriss et al., 1998; Dodd et al., 2012; Moschen et al., 2005).
1013 Shallower areas heat up faster especially in the photic zone. The temperature profile
1014 near to the western shoreline taken in August 2012 (Fig. 6) shows 12°C at the surface
1015 with an average of app. 10°C in the first 15m of the water column decreasing to app.
1016 6°C in 30m depth. Although a spatial difference of 5°C in the photic zone for causing
1017 a 1‰ shift is rather unlikely, this could account for part of the variation in surface
1018 $\delta^{18}\text{O}_{\text{diatom}}$.

1019
1020

1021 **5.3 Factors explaining the spatial chironomid distribution**

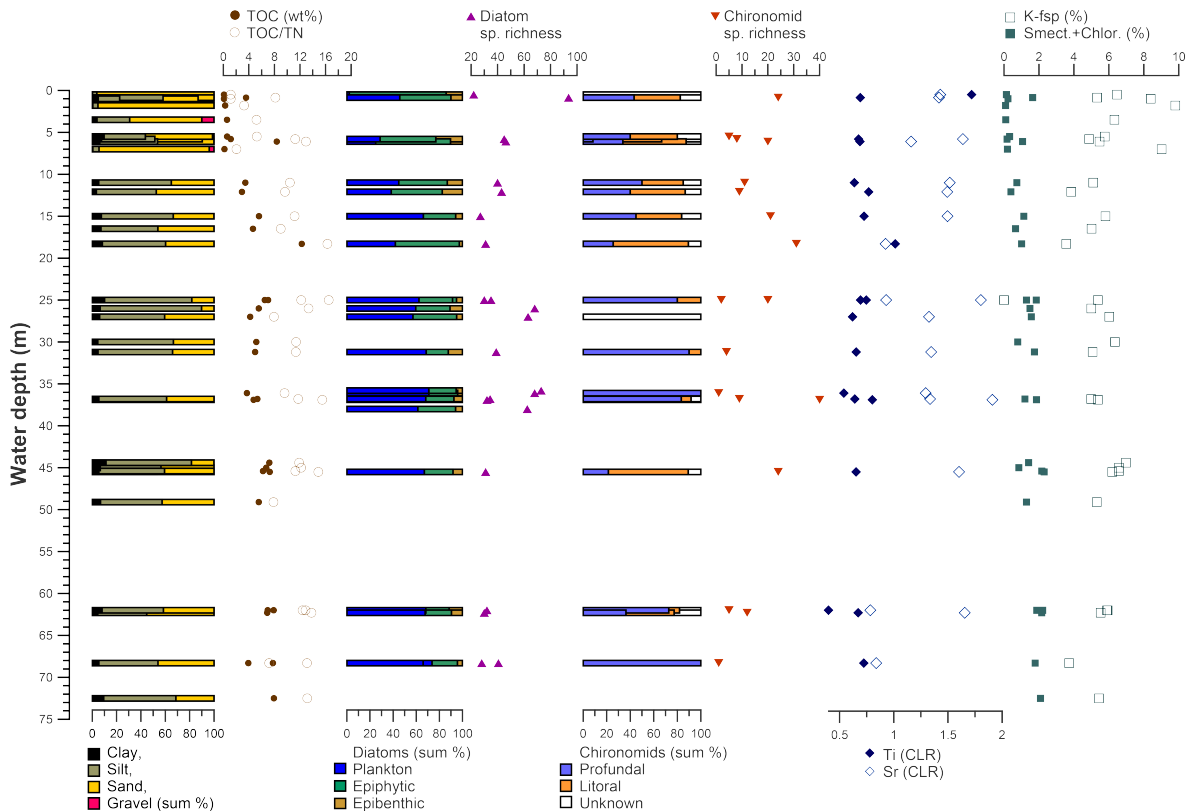
1022 The chironomid RDA indicates that spatial variations are primarily influenced by
1023 the distribution of tributary rivers. For example, high species diversity is found
1024 adjacent to the Utuk river inflow (2117), and in the SE lagoon fed from a small
1025 inflowing stream (PG2122). Semiterrestrial taxa, like *Smittia-Parasmittia*,
1026 *Pseudosmittia*, *Limnophies-Paralimnophies*, have been found only here with the
1027 highest abundancies of 6 and 3.2% at the sites opposite of the inflowing rivers
1028 (PG2117 and PG2122) suggesting these taxa were transported from marshy river
1029 deltas.

1030 Species at lentic sites with no tributary influence are primarily controlled by water
1031 depth. Deep profundal sites of the lake have much lower taxonomic richness of
1032 chironomid communities. Higher taxonomic richness at site PG2118 can be explained
1033 by an enriching riverine influence. High proportions of lotic and lotic-lentic taxa lead
1034 to a high taxonomic similarity of this profundal site to littoral sites in the S and SE.
1035 Similarly, in relation to temperature, sublittoral and profundal sites both have much
1036 higher representation of the taxa characteristic of semi-warm conditions and lower
1037 abundancies of the taxa preferring warm and cold conditions. However, high depths
1038 of the sublittoral and profundal sites lead to the development of a poor chironomid
1039 fauna at these sites. High distance from the shore and presumably only weak
1040 transportation of chironomid remains of littoral fauna to the profundal zone could be
1041 another limiting factor for diversity of chironomid communities in the profundal.

1042 Eastern relatively shallow littorals are inhabited by more diverse, phytophilic,
1043 mesotrophic and partly acidophilic fauna with absence of lotic taxa, related to a less
1044 disturbed and turbulent environments and presence of macrophytes. This fauna has
1045 higher abundance of the semi-warm and warm taxa. The presence of meso- to
1046 eutrophic and acidophilic taxa can be attributed to paludification of the shore zone
1047 and decomposition of macrophytes and submerged vegetation in the shallow littoral
1048 (Nazarova et al., 2017b).

1049 It is still debated how spatial and local environmental processes influence the
1050 distribution of chironomids at a small spatial scale in a lake (Luoto and Ojala,
1051 2018; Yang et al., 2017). It is known that within one water body the concentration of
1052 chironomid head capsules can vary from zero to several thousand per 1 cm³ of
1053 sediments (Kalinkina and Belkina, 2018; Walker et al., 1997) depending on factors
1054 such as water depth, rate of sediment accumulation, the hydrological conditions, or
1055 anthropogenic influence. Water depth in particular is a major driving factor of
1056 chironomid assemblages (Ali et al., 2002; Luoto, 2012; Vemeaux and Aleya, 1998) with
1057 depth optima of several species consistent across broad spatial scales (Nazarova et
1058 al., 2011). Chironomid remains from the deepest zones of Bolshoe Toko represents
1059 an assemblage of elements of profundal necrocenosis (Hofmann, 1971) mixed with
1060 secondary components of littoral fauna transported with in-lake hydrological and

1061 sedimentary processes into the profundal from outside. Thus, the re-deposition of
 1062 littoral taxa into the profundal zone is an important factor that affects the final
 1063 composition and abundance of subfossil assemblages. While in small lakes, subfossil
 1064 assemblages from the profundal zone quite adequately reflect the fauna of the entire
 1065 water body (Brooks and Birks, 2001; Walker and Mathewes, 1990), our findings
 1066 support the hypothesis that in large lakes the taphonomy of chironomid communities
 1067 seems to be more complex (Yang et al., 2017; Árvá et al., 2015).
 1068
 1069



1070
 1071 **Fig. 12** Distribution of grain size, organic carbon and nitrogen indices, diatom and chironomid parameters, and
 1072 selected elements and minerals in dependence to water depth in lake Bolshoe Toko.
 1073

1074 **5.4 Lake Bolshoe Toko as a site for palaeoclimate reconstructions**

1075 Compared to small lowland lakes of Central and Northern Yakutia, sedimentary
 1076 processes are quite different in Bolshoe Toko. One reason is the lack of thaw slumps,
 1077 subsidence, and other permafrost related phenomena (Biskaborn et al., 2013b) that
 1078 are typical for shallow thermokarst lake settings across northern permafrost regions
 1079 (Biskaborn et al., 2016; Bouchard et al., 2016; Biskaborn et al., 2012; Schleusner et al.,
 1080 2015; Biskaborn et al., 2013a; Subetto et al., 2017; Biskaborn et al., 2013b).

1081 The Bolshoe Toko mineral composition is primarily influenced by the Utuk river,
 1082 and only samples in extremely shallow areas are influenced by direct shoreline input.

1083 The grain-size signal is influenced by dissolution effects associated with organic
1084 matter and *in situ* growth of diatom valves. Conversely, the coarser fractions parallel
1085 minerogenic compositions and water depth. Accordingly, the grain-size distribution
1086 originated from multiple processes and should only be considered as an
1087 environmental proxy when combined with biotic indicators.

1088 Diatoms are spatially distributed according to their preferred habitat. Aside from
1089 the spatial habitat conditions associated with basin morphology, an additional
1090 consideration is the annual duration and thickness of lake ice-cover (Keatley et al.,
1091 2008;Smol, 1988a). For instance, planktonic communities in Lake Baikal, including
1092 *Aulacoseira* species, are found to grow under the ice if the surface snow properties
1093 (i.e. thickness, density) allow sufficient light penetration (Jewson et al., 2009;Mackay
1094 et al., 2005). Generally, planktonic and benthic diatom species have strategies to
1095 survive in ice-covered lakes by growing in benthic mode, forming resting spores, or
1096 attaching to the ice-cover substrate (D'souza, 2012). Hence, the duration and
1097 presence of ice-cover can significantly impact both changes in assemblage
1098 composition and spatial distribution, particularly including the ratio of planktonic to
1099 benthic diatoms (Wang et al., 2012a;Bailey et al., 2018).

1100 The applicability of chironomids for temperature reconstructions reveals clear
1101 spatial constraints. 22% of the taxa in sites with riverine influence are absent or rare
1102 from the FE mean July chironomid-based temperature inference model (Nazarova et
1103 al., 2015), whereas fewer of these rare/absent taxa occur in the central and northern
1104 littoral, sublittoral and profundal part of the lake (Fig. 4). However, low taxonomic
1105 richness of the profundal zone also hampers palaeoclimatic inferences. Also the
1106 number of chironomid head capsules are generally lower here relative to littoral sites.
1107 Maximum taxonomic diversity in areas influenced by lake tributaries can be explained
1108 by both a taxonomic enrichment from the lake catchment, as well by more favorable
1109 oxygen and nutrient conditions.

1110 The applicability of $\delta^{18}\text{O}_{\text{diatom}}$ as a proxy of past hydroclimate conditions at
1111 Bolshoe Toko is facilitated by the main controls influencing on $\delta^{18}\text{O}_{\text{diatom}}$, which are
1112 here found to be: (1) lake water temperature (T_{lake}) and (2) lake water isotope
1113 composition ($\delta^{18}\text{O}_{\text{lake}}$) (Dodd and Sharp, 2010;Leng and Barker, 2006;Labeyrie,
1114 1974;Leclerc and Labeyrie, 1987). The fractionation between lake water and biogenic
1115 opal can be calculated when comparing $\delta^{18}\text{O}_{\text{lake}}$ (mean: -18.7‰) with recent surface
1116 sediments of Bolshoe Toko lake and their respective mean $\delta^{18}\text{O}_{\text{diatom}}$ (of $+22.8\text{‰}$)
1117 using this isotope fractionation correlation between sedimentary diatom silica and
1118 water as determined by Leclerc and Labeyrie (1987). The mean T_{lake} can be estimated
1119 to ca. 6°C for the photic zone/diatom bloom. This estimate is at the lower end of
1120 summer temperatures between 4.8 and 12°C . The corresponding derived mean
1121 isotope fractionation factor for the system diatom silica–water $\alpha = 1.0424$ matches the

1122 fractionation factor for sediments proposed by Juillet-Leclerc and Labeyrie (1987) well
1123 ($\alpha_{(\text{silica-water})} = 1.0432$).

1124 Additionally, as lacustrine $\delta^{18}\text{O}_{\text{diatom}}$ also reflects the isotopic composition of the
1125 water where the diatoms grow ($\delta^{18}\text{O}_{\text{lake}}$), $\delta^{18}\text{O}_{\text{diatom}}$ typically reflects meteoric inputs
1126 associated with precipitation and riverine inflows (Fig. 6b). For example, existing
1127 studies have used lacustrine $\delta^{18}\text{O}_{\text{diatom}}$ to reconstruct past changes in precipitation
1128 amount and seasonality, the precipitation/evaporation balance, spring snow melt
1129 inputs, and synoptic-scale shifts in atmospheric circulation (Bailey et al., 2015; Meyer
1130 et al., 2015; Bailey et al., 2018; Kostrova et al., 2013; Mackay et al., 2013). It is
1131 envisaged that changes in $\delta^{18}\text{O}_{\text{diatom}}$ through time at a single site in Bolshoe Toko will
1132 yield insights into the long-term air temperature and palaeohydrological history of the
1133 region.

1134 Positive feedback mechanisms between benthic algae and chironomid larvae in
1135 benthic ecosystems are well-documented (Herren et al., 2017). Chironomids in
1136 Bolshoe Toko, however, showed less significant correlations with benthic diatom
1137 species, but weak correlations with planktonic species and lake attributes associated
1138 to benthic habitats and water depth, highlighting the potential of chironomids for
1139 independent water depth and temperature reconstruction in future sediment core
1140 studies (Nazarova et al., 2011).

1141 High correlation coefficients between organic carbon and *Pliocaenicus*
1142 *bolshetokoensis* (0.66) and silt (0.65) suggest that the accumulation of organic matter
1143 and intermediate grain-size fraction is, to a certain degree, controlled by the
1144 productivity of siliceous microalgae (Biskaborn et al., 2012). A strong contribution of
1145 plankton indicates that TOC/TN ratios can provide insights in the relative influx
1146 between land and water plants (Meyers and Teranes, 2002). The relatively weak
1147 correlation between TOC/TN ratios and water depth (0.51 r), demonstrates the
1148 accuracy limits of TOC/TN as a proxy for relative lake level changes. This is caused
1149 by transport and accumulation of allochthonous organic matter in proximity to the Utuk
1150 river. Furthermore, correlations between TOC/TN and TOC, as well as negative
1151 correlations with grain size indicators suggest diagenetic alteration (i.e. loss) of
1152 nitrogen in the surface sediments (Galman et al., 2008).

1153 The distinct difference between two samples along the subaquatic slope near the
1154 western shore (diatoms, minerals, organics) indicates redistribution of sediment.
1155 Downslope transport of surface layers over the time could lead to redistribution of old
1156 material into the deepest parts of the basin. Due to higher accumulation rates, a
1157 sediment core from the deepest part of the basin would potentially provide a higher
1158 temporal resolution, but also a higher risk of repositioned sediment layers. On top of
1159 redistribution processes, hump-shaped relations between lake depth and species
1160 diversity observed in other studies suggest that the total subfossil species
1161 assemblages is better represented at intermediate depths than at the maximum depth

1162 (Raposeiro et al., 2018). A coring site at intermediate depth in the shallow northern
1163 and sedimentologically calm sector of the basin would enable the tracking of different
1164 river and glacial influences, and offers greater chances of undisturbed successions of
1165 bioindicator time series.
1166

1167 **6 Conclusions**

1168 Our study on the within-lake variance of environmental indicator data and its
1169 attribution to habitat factors improves the understanding of lake-internal filters
1170 between environmental forcing and the resulting sediment parameters of Lake
1171 Bolshoe Toko and comparable boreal, cold, and deep lakes. We found that the spatial
1172 variabilities of biotic ecosystem components are mainly explained by static habitat
1173 preferences as water depth and river distance. Abiotic sediment features are not
1174 symmetrically distributed in the basin but vary along restricted areas of differential
1175 environmental forcings (e.g. river input, rocky shore, steep shore, shallow shore).
1176 They depend, in addition to water depth and riverine activity, to multiple interacting
1177 factor, such as catchment characteristics, geochemical sediment diagenesis and
1178 hydrochemical dynamics. Our main findings can be highlighted as follows:
1179

- 1180 • The lake water of Bolshoe Toko can be characterized as Ca-Mg-HCO₃-Type
1181 water. It is well saturated in O₂, neutral to slightly acidic, showing a low
1182 conductivity and corresponding ion concentrations suggesting unpolluted
1183 freshwater conditions. Lake Bolshoe Toko is a cold, polymictic, oligotrophic,
1184 open through-flow lake system and can be regarded as an undisturbed
1185 ecosystem.
- 1186 • Water depth is a strong factor explaining the spatial variability of diatoms and
1187 chironomids. The proportions of planktonic to benthic diatoms and profundal
1188 to littoral chironomids serve as a reliable lake level proxy.
- 1189 • The diatom assemblage is dominated by planktonic species, i.e. *Pliocaenicus*
1190 *bolshetokoensis*, which is unique for this lake, and more common plankton
1191 such as *Cyclotella* and *Aulacoseira*, as well as non-planktonic taxa, such as
1192 *Achnantheidium*. Diatom species richness and diversity is higher in surface
1193 sediments in the northern part of the basin, associated to shallower waters and
1194 the availability of benthic and periphytic niches.
- 1195 • The $\delta^{18}\text{O}_{\text{diatom}}$ values ($22.8 \pm 0.6\text{‰}$) show slight spatial variations with higher
1196 values in the deeper south-western part of the lake probably related to water
1197 temperature differences in the photic zone during the main diatom bloom. The
1198 silica–water isotope fractionation is suitable for further downcore investigations
1199 for assessing palaeohydrological information and potential air-temperature
1200 changes in the region.

- 1201
- 1202
- 1203
- 1204
- 1205
- 1206
- 1207
- 1208
- 1209
- 1210
- 1211
- 1212
- 1213
- 1214
- 1215
- 1216
- 1217
- 1218
- 1219
- 1220
- 1221
- 1222
- 1223
- 1224
- 1225
- 1226
- 1227
- 1228
- 1229
- 1230
- 1231
- 1232
- The water of Bolshoe Toko is well mixed and does not show significant isotopic stratification apart from lake ice-cover formation where thermal stratification prevents mixing. The isotopic lake water composition ($\delta^{18}\text{O} = 18.2 \pm 0.2 \text{ ‰}$) correspond with the GMWL and do not show evaporative enrichment. Both isotopic and hydrochemical data indicate atmospheric precipitation (and meltwater run-off) as the main water source. Accordingly, $\delta^{18}\text{O}_{\text{lakewater}}$ is directly linked to $\delta^{18}\text{O}_{\text{precipitation}}$.
 - The highest amount of the chironomid taxa underrepresented in the FE training set used for regional palaeoclimate inference was found close to the Utuk river and at southern littoral and profundal sites. Poor chironomid communities from the deep profundal zone would also hamper palaeoclimate reconstruction. Cold-stenotherm chironomid taxa were influenced by river proximity while taxa preferring warm conditions were more frequent at shallow littorals of the lake.
 - Weak negative correlation between mean grain size and water depth is explain by end-members revealing influences of river input and diatom valves in the grain-size composition.
 - Observed TOC values (mean 4.9 %) and TOC/TN ratios indicate strong allochthonous supply of organic matter from the Utuk river. $\delta^{13}\text{C}$ (mean -26.8 ‰) indicate dominance of C_3 plants and phytoplankton in the bulk organic matter fraction. Radiocarbon dating suggests that there is a reservoir effect caused by input of old organic carbon by max. $720 \pm 30 \text{ }^{14}\text{C}$ yrs BP.
 - Elemental (XRF) data and mineral (XRD) distribution is influenced by the methamorphic lithology of the Stanovoy mountain range. Ratios of minerals relative to quartz decrease from the Utuk river towards the northern lake basin. Ti correlates well with mean grain size. There is no clear pattern in Mn/Fe ratios, due to mixture of allochthonous elements and differential intensities of redox processes in the lake basin.
 - The observed proxy variabilities in the surface sediments suggest at least two locations for sediment coring: (1) at intermediate depth in the northern basin to account for representative bioindicator distributions, and (2) the deep part in the central basin to potentially receive higher temporal resolution in the sedimentary record.

1233

1234 **Data Availability**

1235 All data used in this study will be available online at PANGAEA.

1236

1237 **Supplement**

1238 The supplementary material related to this study will be available online at
1239 Copernicus.

1240 **Author contributions**

1241 BKB conceived the study, led the laboratory analyses and the writing of the
1242 manuscript. LN conducted statistical analyses and contributed with ecological
1243 chironomid expertise. LAP led the Russian team during field work and contributed
1244 with ecological diatom expertise. LS conducted chironomid analysis. KF conducted
1245 diatom analyses. HM conducted water chemistry analyses. BC and HLB analysed
1246 diatom opal oxygen isotopes. SV conducted the XRF analysis. RG and EZ retrieved
1247 surface samples during field work and helped with translation of Russian literature
1248 and geographical expertise of the study area. RW conducted grain-size analyses
1249 including end-member modelling. GS conducted XRD analyses. BD was the leader
1250 of German expedition team and contributed with sedimentological expertise.
1251

1252 **Competing interests**

1253 The authors declare that they have no conflict of interest.

1254 **Acknowledgements**

1255 The expedition Yakutia 2013 was financed and conducted by the Alfred Wegener
1256 Institute Helmholtz Centre for Polar and Marine Research in Potsdam, Germany in
1257 collaboration with the North Eastern Federal University in Yakutsk, Russia. Parts of
1258 the study was financed by the Federal Ministry of Education and Research (BMBF) in
1259 the PALMOD project (#01LP1510D) and grant #5.2711.2017/4.6, the Russian
1260 Foundation for Basic Research (RFBR grant #18-45-140053 r_a), and the Project of
1261 the North-Eastern Federal University (Regulation SMK-P-1/2-242-17 ver. 2.0, order
1262 No. 494-OD), Russian Science Foundation (#16-17-10118), and Deutsche
1263 Forschungsgemeinschaft DFG (#NA 760/5-1 and #DI 655/9-1). We thank Almut
1264 Dressler and Clara Biskaborn for help with diatom microscopy and Thomas Löffler for
1265 help with mineral analyses. We thank Emilie Saulnier-Talbot and Anson Mackay for
1266 their voluntary efforts to assure the quality of this study.
1267
1268

1269 **References**

1270 Adrian, R., O'Reilly, C. M., Zagarese, H., Baines, S. B., Hessen, D. O., Keller, W., Livingstone, D. M.,
1271 Sommaruga, R., Straile, D., Van Donk, E., Weyhenmeyer, G. A., and Winder, M.: Lakes as sentinels
1272 of climate change, *Limnology and Oceanography*, 54, 2283-2297,
1273 10.4319/lo.2009.54.6_part_2.2283, 2009.

- 1274 Ali, A., Frouz, J., and Lobinske, R. J.: Spatio-temporal effects of selected physico-chemical variables
1275 of water, algae and sediment chemistry on the larval community of nuisance Chironomidae (Diptera)
1276 in a natural and a man-made lake in central Florida, *Hydrobiologia*, 470, 181-193, 2002.
- 1277 AMAP: Snow, Water, Ice and Permafrost in the Arctic (SWIPA) 2017, Oslo, Norway, 1-269, 2017.
- 1278 Anderson, N. J.: Variability of diatom concentrations and accumulation rates in sediments of a small
1279 lake basin, *Limnology and Oceanography*, 35, 497-508, 1990.
- 1280 Anderson, N. J., Korsman, T., and Renberg, I.: Spatial heterogeneity of diatom stratigraphy in varved
1281 and non-varved sediments of a small, boreal-forest lake, *Aquatic Sciences*, 56, 40-58,
1282 10.1007/bf00877434, 1994.
- 1283 Anderson, N. J.: Diatoms, temperature and climatic change, *European Journal of Phycology*, 35,
1284 307-314, doi:null, 2000.
- 1285 Árva, D., Tóth, M., Horváth, H., Nagy, S. A., and Specziár, A.: The relative importance of spatial and
1286 environmental processes in distribution of benthic chironomid larvae within a large and shallow lake,
1287 *Hydrobiologia*, 742, 249-266, 2015.
- 1288 Bailey, H. L., Henderson, A. C. G., Sloane, H. J., Snelling, A., Leng, M. J., and Kaufman, D. S.: The
1289 effect of species on lacustrine δ 18O diatom and its implications for palaeoenvironmental
1290 reconstructions, *Journal of Quaternary Science*, 29, 393-400, 10.1002/jqs.2711, 2014.
- 1291 Bailey, H. L., Kaufman, D. S., Henderson, A. C. G., and Leng, M. J.: Synoptic scale controls on the
1292 δ 18O in precipitation across Beringia, *Geophysical Research Letters*, 42, 4608-4616,
1293 10.1002/2015GL063983, 2015.
- 1294 Bailey, H. L., Kaufman, D. S., Sloane, H. J., Hubbard, A. L., Henderson, A. C. G., Leng, M. J., Meyer,
1295 H., and Welker, J. M.: Holocene atmospheric circulation in the central North Pacific: A new terrestrial
1296 diatom and δ 18O dataset from the Aleutian Islands, *Quaternary Science Reviews*, 194, 27-38,
1297 10.1016/j.quascirev.2018.06.027, 2018.
- 1298 Barinova, S., Nevo, E., and Bragina, T.: Ecological assessment of wetland ecosystems of northern
1299 Kazakhstan on the basis of hydrochemistry and algal biodiversity, 2011.
- 1300 Battarbee, R. W., and Kneen, M. J.: The use of electronically counted microspheres in absolute
1301 diatom analysis, *Limnology and Oceanography*, 27, 184-188, 1982.
- 1302 Battarbee, R. W., Jones, V. J., Flower, R. J., Cameron, N. G., Bennion, H., Carvalho, L., and
1303 Juggins, S.: Diatoms, in: *Tracking Environmental Change Using Lake Sediments*, edited by: Smol, J.
1304 P., Birks, H. J. B., and Last, W. M., Kluwer Academic Publishers, Dordrecht, Netherlands, 155-202,
1305 2001.
- 1306 Bennion, H., Sayer, C. D., Tibby, J., and Carrick, H. J.: Diatoms as Indicators of Environmental
1307 Change in Shallow Lakes, in: *The Diatoms: Application for the Environmental and Earth Sciences*,
1308 edited by: Smol, J. P., and Stoermer, E. F., Cambridge University Press, Cambridge, 152-173, 2010.
- 1309 Birks, H. J. B.: Quantitative palaeoenvironmental reconstructions, *Statistical modelling of quaternary
1310 science data. Technical guide*, 5, 161-254, 1995.
- 1311 Biskaborn, B., Herzschuh, U., Bolshiyarov, D., Savelieva, L., Zibulski, R., and Diekmann, B.: Late
1312 Holocene thermokarst variability inferred from diatoms in a lake sediment record from the Lena Delta,
1313 Siberian Arctic, *Journal of Paleolimnology*, 49, 155-170, 10.1007/s10933-012-9650-1, 2013a.

- 1314 Biskaborn, B., Herzschuh, U., Bolshiyarov, D., Schwamborn, G., and Diekmann, B.: Thermokarst
1315 Processes and Depositional Events in a Tundra Lake, Northeastern Siberia, Permafrost and
1316 Periglacial Processes, 24, 160-174, 10.1002/ppp.1769, 2013b.
- 1317 Biskaborn, B. K., Herzschuh, U., Bolshiyarov, D., Savelieva, L., and Diekmann, B.: Environmental
1318 variability in northeastern Siberia during the last similar to 13,300 yr inferred from lake diatoms and
1319 sediment-geochemical parameters, *Palaeogeography Palaeoclimatology Palaeoecology*, 329, 22-36,
1320 10.1016/j.palaeo.2012.02.003, 2012.
- 1321 Biskaborn, B. K., Subetto, D. A., Savelieva, L. A., Vakhrameeva, P. S., Hansche, A., Herzschuh, U.,
1322 Klemm, J., Heinecke, L., Pestryakova, L. A., Meyer, H., Kuhn, G., and Diekmann, B.: Late
1323 Quaternary vegetation and lake system dynamics in north-eastern Siberia: Implications for seasonal
1324 climate variability, *Quaternary Science Reviews*, 147, 406-421, 10.1016/j.quascirev.2015.08.014,
1325 2016.
- 1326 Biskaborn, B. K., Smith, S. L., Noetzi, J., Matthes, H., Vieira, G., Streletskiy, D. A., Schoeneich, P.,
1327 Romanovsky, V. E., Lewkowicz, A. G., Abramov, A., Allard, M., Boike, J., Cable, W. L., Christiansen,
1328 H. H., Delaloye, R., Diekmann, B., Drozdov, D., Etzelmüller, B., Grosse, G., Guglielmin, M.,
1329 Ingeman-Nielsen, T., Isaksen, K., Ishikawa, M., Johansson, M., Johannsson, H., Joo, A., Kaverin, D.,
1330 Kholodov, A., Konstantinov, P., Kröger, T., Lambiel, C., Lanckman, J.-P., Luo, D., Malkova, G.,
1331 Meiklejohn, I., Moskalenko, N., Oliva, M., Phillips, M., Ramos, M., Sannel, A. B. K., Sergeev, D.,
1332 Seybold, C., Skryabin, P., Vasiliev, A., Wu, Q., Yoshikawa, K., Zheleznyak, M., and Lantuit, H.:
1333 Permafrost is warming at a global scale, *Nature Communications*, 10, 264, 10.1038/s41467-018-
1334 08240-4, 2019.
- 1335 Bouchard, F., Turner, K. W., MacDonald, L. A., Deakin, C., White, H., Farquharson, N., Medeiros, A.
1336 S., Wolfe, B. B., Hall, R. I., Pienitz, R., and Edwards, T. W. D.: Vulnerability of shallow subarctic
1337 lakes to evaporate and desiccate when snowmelt runoff is low, *Geophysical Research Letters*, 40,
1338 6112-6117, 10.1002/2013gl058635, 2013.
- 1339 Bouchard, F., MacDonald, L. A., Turner, K. W., Thienpont, J. R., Medeiros, A. S., Biskaborn, B. K.,
1340 Korosi, J., Hall, R. I., Pienitz, R., and Wolfe, B. B.: Paleolimnology of thermokarst lakes: a window
1341 into permafrost landscape evolution, *Arctic Science*, 10.1139/AS-2016-0022, 2016.
- 1342 Bracht-Flyr, B., and Fritz, S. C.: Synchronous climatic change inferred from diatom records in four
1343 western Montana lakes in the U.S. Rocky Mountains, *Quaternary Research*, 77, 456-467,
1344 10.1016/j.yqres.2011.12.005, 2012.
- 1345 Brandriss, M. E., O'Neil, J. R., Edlund, M. B., and Stoermer, E. F.: Oxygen Isotope Fractionation
1346 Between Diatomaceous Silica and Water, *Geochimica et Cosmochimica Acta*, 62, 1119-1125,
1347 10.1016/S0016-7037(98)00054-4, 1998.
- 1348 Brooks, S. J., and Birks, H. J. B.: Chironomid-inferred air temperatures from Lateglacial and
1349 Holocene sites in north-west Europe: progress and problems, *Quaternary Science Reviews*, 20,
1350 1723-1741, 2001.
- 1351 Brooks, S. J., Langdon, P. G., and Heiri, O.: The identification and use of Palaeartic Chironomidae
1352 larvae in palaeoecology, *Quaternary Research Association*, 2007.
- 1353 Chaplign, B., Meyer, H., Friedrichsen, H., Marent, A., Sohns, E., and Hubberten, H. W.: A high-
1354 performance, safer and semi-automated approach for the $\delta^{18}\text{O}$ analysis of diatom silica and new
1355 methods for removing exchangeable oxygen, *Rapid Communications in Mass Spectrometry*, 24,
1356 2655-2664, 2010.
- 1357 Chaplign, B.: From method development to climate reconstruction - oxygen isotope analysis of
1358 biogenic silica from Lake El'gygytgyn, NE Siberia, PhD thesis, Alfred Wegener Institute for Polar and
1359 Marine Research, University of Potsdam, Potsdam, 196 pp., 2011.

- 1360 Chaplign, B., Meyer, H., Bryan, A., Snyder, J., and Kemnitz, H.: Assessment of purification and
1361 contamination correction methods for analysing the oxygen isotope composition from biogenic silica,
1362 *Chemical Geology*, 300, 185-199, 10.1016/j.chemgeo.2012.01.004, 2012a.
- 1363 Chaplign, B., Meyer, H., Swann, G. E. A., Meyer-Jacob, C., and Hubberten, H. W.: A 250 ka oxygen
1364 isotope record from diatoms at Lake El'gygytgyn, far east Russian Arctic, *Climate of the Past*, 8,
1365 1621-1636, 2012b.
- 1366 Cohen, A. S.: *Palaeolimnology - The History and Evolution of Lake Systems*, Oxford University
1367 Press, Oxford, 500 pp., 2003.
- 1368 Colquhoun, D.: An investigation of the false discovery rate and the misinterpretation of p-values, *Roy
1369 Soc Open Sci*, 1, ARTN 140216
1370 10.1098/rsos.140216, 2014.
- 1371 Cremer, H., and Van de Vijver, B.: On *Pliocaenicus costatus* (Bacillariophyceae) in Lake El'gygytgyn,
1372 East Siberian, *European Journal of Phycology*, 41, 169-178, 10.1080/09670260600621932, 2006.
- 1373 D'souza, N. A.: *Psychrophilic diatoms in ice-covered lake Erie*, Bowling Green State University, 158
1374 pp., 2012.
- 1375 Dansgaard, W.: *Stable Isotopes in Precipitation*, *Tellus*, 16, 436-468, 1964.
- 1376 Dietze, E., Hartmann, K., Diekmann, B., Ijmker, J., Lehmkuhl, F., Opitz, S., Stauch, G., Wünnemann,
1377 B., and Borchers, A.: An end-member algorithm for deciphering modern detrital processes from lake
1378 sediments of Lake Donggi Cona, NE Tibetan Plateau, China, *Sedimentary Geology*, 243-244, 169-
1379 180, 10.1016/j.sedgeo.2011.09.014, 2012.
- 1380 Dodd, J. P., and Sharp, Z. D.: A laser fluorination method for oxygen isotope analysis of biogenic
1381 silica and a new oxygen isotope calibration of modern diatoms in freshwater environments,
1382 *Geochimica et Cosmochimica Acta*, 74, 1381-1390, 2010.
- 1383 Dodd, J. P., Sharp, Z. D., Fawcett, P. J., Brearley, A. J., and McCubbin, F. M.: Rapid post-mortem
1384 maturation of diatom silica oxygen isotope values, *Geochemistry, Geophysics, Geosystems*, 13,
1385 10.1029/2011GC004019, 2012.
- 1386 Douglas, M. S. V., and Smol, J. P.: Paleolimnological Significance of observed Distribution Patterns of
1387 Chrysophyte Cysts in Arctic Pond Environments, *Journal of Paleolimnology*, 13, 79-83, 1995.
- 1388 Douglas, M. S. V., and Smol, J. P.: Freshwater Diatoms as Indicators of Environmental Change in
1389 the High Arctic, in: *The Diatoms: Application for the Environmental and Earth Sciences*, edited by:
1390 Smol, J. P., and Stoermer, E. F., Cambridge University Press, Cambridge, 249-266, 2010.
- 1391 Earle, J. C., Duthie, H. C., Glooschenko, W. A., and Hamilton, P. B.: Factors affecting the spatial-
1392 distribution of diatoms on the surface sediments of 3 Precambrian shield lakes, *Canadian Journal of
1393 Fisheries and Aquatic Sciences*, 45, 469-478, 10.1139/f88-056, 1988.
- 1394 Elger, K., Biskaborn, B. K., Pampel, H., and Lantuit, H.: Open research data, data portals and data
1395 publication—an introduction to the data curation landscape, *Polarforschung*, 85, 119-133, 2016.
- 1396 Flower, R. J., and Ryves, D. B.: Diatom preservation: differential preservation of sedimentary diatoms
1397 in two saline lakes, *Acta Botanica Croatica*, 68, 381-399, 2009.
- 1398 Galman, V., Rydberg, J., de-Luna, S. S., Bindler, R., and Renberg, I.: Carbon and nitrogen loss rates
1399 during aging of lake sediment: Changes over 27 years studied in varved lake sediment, *Limnology
1400 and Oceanography*, 53, 1076-1082, DOI 10.4319/lo.2008.53.3.1076, 2008.

- 1401 Gavin, D. G., Henderson, A. C. G., Westover, K. S., Fritz, S. C., Walker, I. R., Leng, M. J., and Hu, F.
 1402 S.: Abrupt Holocene climate change and potential response to solar forcing in western Canada,
 1403 Quaternary Science Reviews, 30, 1243-1255, 10.1016/j.quascirev.2011.03.003, 2011.
- 1404 Gavrilova, K.: Climate and Permafrost, Permafrost and Periglacial Processes, 4, 99-111, 1993.
- 1405 Genkal, S., Gabyshev, V., Kulilovskiy, M., and Kuznetsova, I.: Pliocaenicus bolshetokoensis—a new
 1406 species from Lake Bolshoe Toko (Yakutia, Eastern Siberia, Russia), Diatom Research, 1-9, 2018.
- 1407 Gingele, F. X., De Deckker, P., and Hillenbrand, C.-D.: Clay mineral distribution in surface sediments
 1408 between Indonesia and NW Australia—source and transport by ocean currents, Marine Geology,
 1409 179, 135-146, 2001.
- 1410 Gushulak, C. A. C., Laird, K. R., Bennett, J. R., and Cumming, B. F.: Water depth is a strong driver of
 1411 intra-lake diatom distributions in a small boreal lake, Journal of Paleolimnology, 58, 231-241,
 1412 10.1007/s10933-017-9974-y, 2017.
- 1413 Hakanson, L.: Influence of Wind, Fetch, and Water Depth on Distribution of Sediments in Lake
 1414 Vanern, Sweden, Canadian Journal of Earth Sciences, 14, 397-412, 10.1139/e77-040, 1977.
- 1415 Heggen, M. P., Birks, H. H., Heiri, O., Grytnes, J. D., and Birks, H. J. D.: Are fossil assemblages in a
 1416 single sediment core from a small lake representative of total deposition of mite, chironomid, and
 1417 plant macrofossil remains?, Journal of Paleolimnology, 48, 669-691, 2012.
- 1418 Heinecke, L., Mischke, S., Adler, K., Barth, A., Biskaborn, B. K., Plessen, B., Nitze, I., Kuhn, G.,
 1419 Rajabov, I., and Herzsuh, U.: Climatic and limnological changes at Lake Karakul (Tajikistan) during
 1420 the last similar to 29 cal ka, Journal of Paleolimnology, 58, 317-334, 10.1007/s10933-017-9980-0,
 1421 2017.
- 1422 Heiri, O., and Lotter, A. F.: Effect of low count sums on quantitative environmental reconstructions:
 1423 an example using subfossil chironomids, Journal of Paleolimnology, 26, 343-350, 2001.
- 1424 Heiri, O., Brooks, S. J., Renssen, H., Bedford, A., Hazekamp, M., Ilyashuk, B., Jeffers, E. S., Lang,
 1425 B., Kirilova, E., and Kuiper, S.: Validation of climate model-inferred regional temperature change for
 1426 late-glacial Europe, Nature communications, 5, 4914, 2014.
- 1427 Heling, C. L., Stelzer, R. S., Drecktrah, H. G., and Koenigs, R. P.: Spatial variation of benthic
 1428 invertebrates at the whole-ecosystem scale in a large eutrophic lake, Freshwater Science, 37, 605-
 1429 617, 10.1086/699386, 2018.
- 1430 Herren, C. M., Webert, K. C., Drake, M. D., Vander Zanden, M. J., Einarsson, A., Ives, A. R., and
 1431 Gratton, C.: Positive feedback between chironomids and algae creates net mutualism between
 1432 benthic primary consumers and producers, Ecology, 98, 447-455, 10.1002/ecy.1654, 2017.
- 1433 Herzsuh, U., Pestryakova, L. A., Savelieva, L. A., Heinecke, L., Boehmer, T., Biskaborn, B. K.,
 1434 Andreev, A., Ramisch, A., Shinneman, A. L. C., and Birks, H. J. B.: Siberian larch forests and the ion
 1435 content of thaw lakes form a geochemically functional entity, Nature Communications, 4,
 1436 10.1038/ncomms3408, 2013.
- 1437 Hill, M. O.: Diversity and evenness - unifying notation and its consequences, Ecology, 54, 427-432,
 1438 1973.
- 1439 Hilton, J., Lishman, J. P., and Allen, P. V.: The dominant processes of sediment distribution and
 1440 focusing in a small, eutrophic, monomictic lake, Limnology and Oceanography, 31, 125-133, 1986.
- 1441 Hoff, U., Biskaborn, B. K., Dirksen, V. G., Dirksen, O., Kuhn, G., Meyer, H., Nazarova, L., Roth, A.,
 1442 and Diekmann, B.: Holocene environment of Central Kamchatka, Russia: Implications from a multi-

- 1443 proxy record of Two-Yurts Lake, *Global and Planetary Change*, 134, 101-117,
1444 10.1016/j.gloplacha.2015.07.011, 2015.
- 1445 Hofmann, W.: Zur taxonomie und palökologie subfossiler Chironomiden (Dipt.) in seesedimenten,
1446 *Ergebnisse der Limnologie*, 1971.
- 1447 Huang, J., Zhang, X., Zhang, Q., Lin, Y., Hao, M., Luo, Y., Zhao, Z., Yao, Y., Chen, X., Wang, L.,
1448 Nie, S., Yin, Y., Xu, Y., and Zhang, J.: Recently amplified arctic warming has contributed to a
1449 continual global warming trend, *Nature Climate Change*, 7, 875-879, 10.1038/s41558-017-0009-5,
1450 2017.
- 1451 Imaeva, L., Imaev, V., Koz'min, B., and Mackey, K.: Formation dynamics of fault-block structures in
1452 the eastern segment of the Baikal-Stanovoi seismic belt, *Izvestiya-Physics of the Solid Earth*, 45,
1453 1006-1011, 10.1134/S1069351309110081, 2009.
- 1454 Jewson, D. H., Granin, N. G., Zhdanov, A. A., and Gnatovsky, R. Y.: Effect of snow depth on under-
1455 ice irradiance and growth of *Aulacoseira baicalensis* in Lake Baikal, *Aquatic Ecology*, 43, 673-679,
1456 10.1007/s10452-009-9267-2, 2009.
- 1457 Kalinkina, N., and Belkina, N.: Dynamics of benthic communities state and the sediment chemical
1458 composition in Lake Onega under the influence of anthropogenic and natural factors, *Principy*
1459 *èkologii*, 7, 56–74, 10.15393/j1.art.2018.7643, 2018.
- 1460 Kalugin, I., Daryin, A., Smolyaninova, L., Andreev, A., Diekmann, B., and Khlystov, O.: 800-yr-long
1461 records of annual air temperature and precipitation over southern Siberia inferred from Teletskoye
1462 Lake sediments, *Quaternary Research*, 67, 400-410, 10.1016/j.yqres.2007.01.007, 2007.
- 1463 Keatley, B. E., Douglas, M. S. V., and Smol, J. P.: Prolonged ice cover dampens diatom community
1464 responses to recent climatic change in High Arctic lakes, *Arctic Antarctic and Alpine Research*, 40,
1465 364-372, 10.1657/1523-0430(06-068)[keatley]2.0.co;2, 2008.
- 1466 Kienel, U., and Kumke, T.: Combining ordination techniques and geostatistics to determine the
1467 patterns of diatom distributions at Lake Lama, Central Siberia, *Journal of Paleolimnology*, 28, 181-
1468 194, 2002.
- 1469 Kingston, J. C., Lowe, R. L., Stoermer, E. F., and Ladewski, T. B.: Spatial and Temporal Distribution
1470 of Benthic Diatoms in Northern Lake Michigan, *Ecology*, 64, 1566-1580, 10.2307/1937511, 1983.
- 1471 Kloss, A. L.: Water isotope geochemistry of recent precipitation in Central and North Siberia as a
1472 proxy for the local and regional climate system, Diploma thesis, Leibniz University Hannover,
1473 Hannover, Germany, 2008.
- 1474 Konstantinov, A. F.: Problems of Water-Resources Development in Southern Yakutia (in Russian),
1475 *Yaf Sib. Otd. Akad., Nauk SSSR, Yakutsk*, 136 pp., 1986.
- 1476 Konstantinov, A. F.: Environmental problems of lake Bolshoe Toko (in Russian), *Lakes of Cold*
1477 *Environments, part V: Resource Study, Resource Use, Ecology and Nature Protection Issue*,
1478 *Yakutsk, Russia*, 2000, 85-93,
- 1479 Kornilov, B. A.: Relief: The southeast suburbs of Aldan Mountains (in russian), Publishing House of
1480 Academy of Sciences of the USSR, Moscow, 1962.
- 1481 Kostrova, S. S., Meyer, H., Chaplugin, B., Kossler, A., Bezrukova, E. V., and Tarasov, P. E.:
1482 Holocene oxygen isotope record of diatoms from Lake Kotokel (southern Siberia, Russia) and its
1483 palaeoclimatic implications, *Quaternary International*, 290-291, 21-34, 10.1016/j.quaint.2012.05.011,
1484 2013.

- 1485 Kovalenko, K. E., Thomaz, S. M., and Warfe, D. M.: Habitat complexity: approaches and future
1486 directions, *Hydrobiologia*, 685, 1-17, 10.1007/s10750-011-0974-z, 2012.
- 1487 Krammer, K., and Lange-Bertalot, H.: *Bacillariophyceae Band 2/2, Süßwasserflora von Mitteleuropa*,
1488 2, Gustav Fischer Verlag, Stuttgart, 1986-1991.
- 1489 Labeyrie, L.: New approach to surface seawater palaeotemperatures using 18O/16O ratios in silica
1490 of diatom frustules, *Nature*, 248, 40-42, 10.1038/248040a0, 1974.
- 1491 Lange-Bertalot, H., and Metzeltin, D.: Indicators of Oligotrophy, *Iconographia Diatomologica*, 2,
1492 Koeltz Scientific Books, 390 pp., 1996.
- 1493 Lange-Bertalot, H., and Genkal, S. I.: Diatomeen aus Sibirien I, *Iconographia Diatomologica*, 6,
1494 Koeltz Scientific Books, 271 pp., 1999.
- 1495 Lange-Bertalot, H., Hofmann, G., and Werum, M.: *Diatomeen im Süßwasser - Benthos von*
1496 *Mitteleuropa*, Ganter Verlag, 908 pp., 2011.
- 1497 Leclerc, A. J., and Labeyrie, L.: Temperature dependence of the oxygen isotopic fractionation
1498 between diatom silica and water, *Earth and Planetary Science Letters*, 84, 69-74, 1987.
- 1499 Legendre, P., Borcard, D., and Peres-Neto, P. R.: Analyzing beta diversity: Partitioning the spatial
1500 variation of community composition data, *Ecological Monographs*, 75, 435-450, Doi 10.1890/05-
1501 0549, 2005.
- 1502 Leng, M. J., and Barker, P. A.: A review of the oxygen isotope composition of lacustrine diatom silica
1503 for palaeoclimate reconstruction, *Earth-Science Reviews*, 75, 5, 2006.
- 1504 Livingstone, D. M., Lotter, A. F., and Walkery, I. R.: The decrease in summer surface water
1505 temperature with altitude in Swiss Alpine lakes: a comparison with air temperature lapse rates, *Arctic*,
1506 *Antarctic, and Alpine Research*, 31, 341-352, 1999.
- 1507 Luoto, T. P.: Spatial uniformity in depth optima of midges: evidence from sedimentary archives of
1508 shallow Alpine and boreal lakes, *Journal of Limnology*, 71, e24-e24, 2012.
- 1509 Luoto, T. P., and Ojala, A. E. K.: Controls of climate, catchment erosion and biological production on
1510 long-term community and functional changes of chironomids in High Arctic lakes (Svalbard),
1511 *Palaeogeography Palaeoclimatology Palaeoecology*, 505, 63-72, 10.1016/j.palaeo.2018.05.026,
1512 2018.
- 1513 Mackay, A. W., Ryves, D. B., Battarbee, R. W., Flower, R. J., Jewson, D., Rioual, P., and Sturm, M.:
1514 1000 years of climate variability in central Asia: assessing the evidence using Lake Baikal (Russia)
1515 diatom assemblages and the application of a diatom-inferred model of snow cover on the lake,
1516 *Global and Planetary Change*, 46, 281-297, 10.1016/j.gloplacha.2004.09.021, 2005.
- 1517 Mackay, A. W., Swann, G. E. A., Fagel, N., Fietz, S., Leng, M. J., Morley, D., Rioual, P., and
1518 Tarasov, P.: Hydrological instability during the Last Interglacial in central Asia: a new diatom oxygen
1519 isotope record from Lake Baikal, *Quaternary Science Reviews*, 66, 45-54,
1520 10.1016/j.quascirev.2012.09.025, 2013.
- 1521 Melles, M., Brigham-Grette, J., Minyuk, P. S., Nowaczyk, N. R., Wennrich, V., DeConto, R. M.,
1522 Anderson, P. M., Andreev, A. A., Coletti, A., Cook, T. L., Haltia-Hovi, E., Kukkonen, M., Lozhkin, A.
1523 V., Rosén, P., Tarasov, P., Vogel, H., and Wagner, B.: 2.8 Million Years of Arctic Climate Change
1524 from Lake El'gygytgyn, NE Russia, *Science*, 337, 315, 10.1126/science.1222135, 2012.
- 1525 Merlivat, L., and Jouzel, J.: Global climatic interpretation of the deuterium-oxygen 18 relationship for
1526 precipitation, *Journal of Geophysical Research: Oceans*, 84, 5029-5033, 1979.

- 1527 Meyer, D., Tachikawa, T., Kaku, M., Iwasaki, A., Gesch, D., Oimoen, M., Zheng, Z., Danielson, J.,
1528 Krieger, T., and Curtis, W.: ASTER global digital elevation model version 2—summary of validation
1529 results, Japan-US ASTER Science Team, 1-26, 2011.
- 1530 Meyer, H., Schönicke, L., Wand, U., Hubberten, H.-W., and Friedrichsen, H.: Isotope studies of
1531 hydrogen and oxygen in ground ice—experiences with the equilibration technique, *Isotopes in
1532 Environmental and Health Studies*, 36, 133-149, 2000.
- 1533 Meyer, H., Chaplignin, B., Hoff, U., Nazarova, L., and Diekmann, B.: Oxygen isotope composition of
1534 diatoms as Late Holocene climate proxy at Two-Yurts Lake, Central Kamchatka, Russia, *Global and
1535 Planetary Change*, 134, 118-128, 2015.
- 1536 Meyers, P. A., and Teranes, J. L.: Sediment organic matter, in: *Tracking Environmental Change
1537 using Lake Sediments. Volume 2: Physical and Geochemical Methods*, edited by: Last, W. M., and
1538 Smol, J. P., Kluwer Academic Publisher, Dordrecht, 239-269, 2002.
- 1539 Meyers, P. A.: Applications of organic geochemistry to paleolimnological reconstructions: a summary
1540 of examples from the Laurentian Great Lakes, *Organic Geochemistry*, 34, 261-289, 2003.
- 1541 Miller, G. H., Brigham-Grette, J., Alley, R. B., Anderson, L., Bauch, H. A., Douglas, M. S. V.,
1542 Edwards, M. E., Elias, S. A., Finney, B. P., Fitzpatrick, J. J., Funder, S. V., Herbert, T. D., Hinzman,
1543 L. D., Kaufman, D. S., MacDonald, G. M., Polyak, L., Robock, A., Serreze, M. C., Smol, J. P.,
1544 Spielhagen, R., White, J. W. C., Wolfe, A. P., and Wolff, E. W.: Temperature and precipitation history
1545 of the Arctic, *Quaternary Science Reviews*, 29, 1679-1715, DOI: 10.1016/j.quascirev.2010.03.001,
1546 2010.
- 1547 Moschen, R., Lucke, A., and Schleser, G. H.: Sensitivity of biogenic silica oxygen isotopes to
1548 changes in surface water temperature and palaeoclimatology, *Geophysical Research Letters*, 32,
1549 L07708
1550 10.1029/2004gl022167, 2005.
- 1551 Naeher, S., Gilli, A., North, R. P., Hamann, Y., and Schubert, C. J.: Tracing bottom water
1552 oxygenation with sedimentary Mn/Fe ratios in Lake Zurich, Switzerland, *Chemical Geology*, 352,
1553 125-133, 10.1016/j.chemgeo.2013.06.006, 2013.
- 1554 Nazarova, L., Pstryakova, L., Ushnitskaya, L., and Hubberten, H.-W.: Chironomids (Diptera:
1555 Chironomidae) in lakes of central Yakutia and their indicative potential for paleoclimatic research,
1556 *Contemporary Problems of Ecology*, 1, 335, 2008.
- 1557 Nazarova, L., Herzsuh, U., Wetterich, S., Kumke, T., and Pstryakova, L.: Chironomid-based
1558 inference models for estimating mean July air temperature and water depth from lakes in Yakutia,
1559 northeastern Russia, *Journal of Paleolimnology*, 45, 57-71, 10.1007/s10933-010-9479-4, 2011.
- 1560 Nazarova, L., Self, A. E., Brooks, S. J., van Hardenbroek, M., Herzsuh, U., and Diekmann, B.:
1561 Northern Russian chironomid-based modern summer temperature data set and inference models,
1562 *Global and Planetary Change*, 134, 10-25, 2015.
- 1563 Nazarova, L., Grebennikova, T. A., Razjigaeva, N. G., Ganzey, L. A., Belyanina, N. I., Arslanov, K.
1564 A., Kaistrenko, V. M., Gorbunov, A. O., Kharlamov, A. A., and Rudaya, N.: Reconstruction of
1565 Holocene environmental changes in Southern Kurils (North-Western Pacific) based on palaeolake
1566 sediment proxies from Shikotan Island, *Global and Planetary Change*, 159, 25-36, 2017a.
- 1567 Nazarova, L. B., Semenov, V. F., Sabirov, R. M., and Efimov, I. Y.: The state of benthic communities
1568 and water quality evaluation in the Cheboksary Reservoir, *Water Resources*, 31, 316-322, 2004.
- 1569 Nazarova, L. B., Self, A. E., Brooks, S. J., Solovieva, N., Syrykh, L. S., and Dauvalter, V. A.:
1570 Chironomid fauna of the lakes from the Pechora river basin (east of European part of Russian Arctic):

- 1571 Ecology and reconstruction of recent ecological changes in the region, *Contemporary Problems of*
1572 *Ecology*, 10, 350-362, 10.1134/s1995425517040059, 2017b.
- 1573 New, M., Lister, D., Hulme, M., and Makin, I.: A high-resolution data set of surface climate over
1574 global land areas, *Climate research*, 21, 1-25, 2002.
- 1575 Palagushkina, O., Wetterich, S., Biskaborn, B. K., Nazarova, L., Schirrmeister, L., Lenz, J.,
1576 Schwamborn, G., and Grosse, G.: Diatom records and tephra mineralogy in pingo deposits of
1577 Seward Peninsula, Alaska, *Palaeogeography, Palaeoclimatology, Palaeoecology*, 2017.
- 1578 Palagushkina, O. V., Nazarova, L. B., Wetterich, S., and Schirrmeister, L.: Diatoms of modern bottom
1579 sediments in Siberian arctic, *Contemporary Problems of Ecology*, 5, 413-422,
1580 10.1134/s1995425512040105, 2012.
- 1581 Paul, C. A., Rühland, K. M., and Smol, J. P.: Diatom-inferred climatic and environmental changes
1582 over the last 9000 years from a low Arctic (Nunavut, Canada) tundra lake, *Palaeogeography*
1583 *Palaeoclimatology Palaeoecology*, 291, 205-216, 10.1016/j.palaeo.2010.02.030, 2010.
- 1584 Pepin, N., Bradley, R. S., Diaz, H. F., Baraer, M., Caceres, E. B., Forsythe, N., Fowler, H.,
1585 Greenwood, G., Hashmi, M. Z., Liu, X. D., Miller, J. R., Ning, L., Ohmura, A., Palazzi, E., Rangwala,
1586 I., Schoner, W., Severskiy, I., Shahgedanova, M., Wang, M. B., Williamson, S. N., Yang, D. Q., and
1587 Mt Res Initiative, E. D. W. W. G.: Elevation-dependent warming in mountain regions of the world,
1588 *Nature Climate Change*, 5, 424-430, 10.1038/nclimate2563, 2015.
- 1589 Pestryakova, L. A., Herzschuh, U., Wetterich, S., and Ulrich, M.: Present-day variability and
1590 Holocene dynamics of permafrost-affected lakes in central Yakutia (Eastern Siberia) inferred from
1591 diatom records, *Quaternary Science Reviews*, 51, 56-70, 2012.
- 1592 Pestryakova, L. A., Herzschuh, U., Gorodnichev, R., and Wetterich, S.: The sensitivity of diatom taxa
1593 from Yakutian lakes (north-eastern Siberia) to electrical conductivity and other environmental
1594 variables, *Polar Research*, 37, 10.1080/17518369.2018.1485625, 2018.
- 1595 Petschick, R., Kuhn, G., and Gingele, F.: Clay mineral distribution in surface sediments of the South
1596 Atlantic: sources, transport, and relation to oceanography, *Marine Geology*, 130, 203-229, 1996.
- 1597 Pillot, H. K. M. M.: *Chironomidae Larvae of the Netherlands and adjacent lowlands: biology and*
1598 *ecology of the chironomini*, KNNV publishing, 2009.
- 1599 Puusepp, L., and Punning, J. M.: Spatio-temporal variability of diatom assemblages in surface
1600 sediments of Lake Peipsi, *Journal of Great Lakes Research*, 37, 33-40, 10.1016/j.jglr.2010.11.018,
1601 2011.
- 1602 QGIS-Team: QGIS geographic information system, Open Source Geospatial Foundation Project,
1603 2016.
- 1604 R Core Team: R: A language and environment for statistical computing. R Foundation for Statistical
1605 Computing, Vienna, Austria, 2012. ISBN 3-900051-07-0, 2012.
- 1606 Raposeiro, P. M., Saez, A., Giralt, S., Costa, A. C., and Goncalves, V.: Causes of spatial distribution
1607 of subfossil diatom and chironomid assemblages in surface sediments of a remote deep island lake,
1608 *Hydrobiologia*, 815, 141-163, 10.1007/s10750-018-3557-4, 2018.
- 1609 Round, F. E., Crawford, R. M., and Mann, D. G.: *The Diatoms. Biology & Morphology of the Genera*,
1610 Cambridge University Press, Cambridge, 747 pp., 1990.

- 1611 Rühland, K., Priesnitz, A., and Smol, J. P.: Paleolimnological evidence from diatoms for recent
 1612 environmental changes in 50 lakes across Canadian arctic treeline, *Arctic Antarctic and Alpine*
 1613 *Research*, 35, 110-123, 10.1657/1523-0430(2003)035[0110:pefdfr]2.0.co;2, 2003.
- 1614 Rühland, K., Paterson, A. M., and Smol, J. P.: Hemispheric-scale patterns of climate-related shifts in
 1615 planktonic diatoms from North American and European lakes, *Global Change Biology*, 14, 2740-
 1616 2754, 10.1111/j.1365-2486.2008.01670.x, 2008.
- 1617 Rühland, K. M., Paterson, A. M., and Smol, J. P.: Lake diatom responses to warming: reviewing the
 1618 evidence, *Journal of Paleolimnology*, 1-35, DOI: 10.1007/s10933-015-9837-3, 2015.
- 1619 Rundqvist, D. V., and Mitrofanov, F. P.: *Precambrian Geology of the USSR*, 1-528 pp., 1993.
- 1620 Ryves, D., Juggins, S., Fritz, S., and Battarbee, R.: Experimental diatom dissolution and the
 1621 quantification of microfossil preservation in sediments, *Palaeogeography Palaeoclimatology*
 1622 *Palaeoecology*, 172, 99-113, 2001.
- 1623 Saulnier-Talbot, E., Gregory-Eaves, I., Simpson, K. G., Efitre, J., Nowlan, T. E., Taranu, Z. E., and
 1624 Chapman, L. J.: Small Changes in Climate Can Profoundly Alter the Dynamics and Ecosystem
 1625 Services of Tropical Crater Lakes, *Plos One*, 9, ARTN e86561
 1626 10.1371/journal.pone.0086561, 2014.
- 1627 Schleusner, P., Biskaborn, B. K., Kienast, F., Wolter, J., Subetto, D., and Diekmann, B.: Basin
 1628 evolution and palaeoenvironmental variability of the thermokarst lake El'gene-Kyuele, Arctic Siberia,
 1629 *Boreas*, 44, 216-229, 10.1111/bor.12084, 2015.
- 1630 Schuur, E. A. G., McGuire, A. D., Schadel, C., Grosse, G., Harden, J. W., Hayes, D. J., Hugelius, G.,
 1631 Koven, C. D., Kuhry, P., Lawrence, D. M., Natali, S. M., Olefeldt, D., Romanovsky, V. E., Schaefer,
 1632 K., Turetsky, M. R., Treat, C. C., and Vonk, J. E.: Climate change and the permafrost carbon
 1633 feedback, *Nature*, 520, 171-179, 10.1038/nature14338, 2015.
- 1634 Self, A. E., Brooks, S. J., Birks, H. J. B., Nazarova, L., Porinchu, D., Odland, A., Yang, H., and Jones,
 1635 V. J.: The distribution and abundance of chironomids in high-latitude Eurasian lakes with respect to
 1636 temperature and continentality: development and application of new chironomid-based climate-
 1637 inference models in northern Russia, *Quaternary Science Reviews*, 30, 1122-1141,
 1638 10.1016/j.quascirev.2011.01.022, 2011.
- 1639 Semenov, S. G.: Current state of ichthyofauna of Lake Bolshoe Toko, South of Russia-Ecology
 1640 Development, 13, 32-42, 2018.
- 1641 Shahgedanova, M.: Climate at Present and in the Historical Past, in: *The Physical Geography of*
 1642 *Northern Eurasia*, edited by: Shahgedanova, M., Oxford University Press, Oxford, 70-102, 2002.
- 1643 Smith, A. C., Leng, M. J., Swann, G. E. A., Barker, P. A., Mackay, A. W., Ryves, D. B., Sloane, H. J.,
 1644 Chenery, S. R. N., and Hems, M.: An experiment to assess the effects of diatom dissolution on
 1645 oxygen isotope ratios, *Rapid Communications in Mass Spectrometry*, 30, 293-300,
 1646 10.1002/rcm.7446, 2016.
- 1647 Smol, J. P.: The Statospore of *Mallomonas Pseudocoronata* (Mallomonadaceae, Chrysophyceae),
 1648 *Nord J Bot*, 4, 827-831, DOI 10.1111/j.1756-1051.1984.tb02014.x, 1984.
- 1649 Smol, J. P., Charles, D. F., and Whitehead, D. R.: Mallomonadacean Microfossils Provide Evidence
 1650 of Recent Lake Acidification, *Nature*, 307, 628-630, DOI 10.1038/307628a0, 1984.
- 1651 Smol, J. P., and Boucherle, M. M.: Postglacial changes in algal and cladoceran assemblages in Little
 1652 Round Lake, Ontario, *Archiv Fur Hydrobiologie*, 103, 25-49, 1985.

- 1653 Smol, J. P.: Paleoclimate proxy data from freshwater arctic diatoms, *Verh. Internat. Verein. Limnol.*,
1654 23, 837-844, 1988a.
- 1655 Smol, J. P.: Chrysophycean microfossils in paleolimnological studies, *Palaeogeography*
1656 *Palaeoclimatology Palaeoecology*, 62, 287-297, 1988b.
- 1657 Smol, J. P., Wolfe, A. P., Birks, H. J. B., Douglas, M. S. V., Jones, V. J., Korhola, A., Pienitz, R.,
1658 Rühland, K., Sorvari, S., Antoniades, D., Brooks, S. J., Fallu, M. A., Hughes, M., Keatley, B. E.,
1659 Laing, T. E., Michelutti, N., Nazarova, L., Nyman, M., Paterson, A. M., Perren, B., Quinlan, R.,
1660 Rautio, M., Saulnier-Talbot, E., Siitonen, S., Solovieva, N., and Weckstrom, J.: Climate-driven
1661 regime shifts in the biological communities of arctic lakes, *Proceedings of the National Academy of*
1662 *Sciences of the United States of America*, 102, 4397-4402, 10.1073/pnas.0500245102, 2005.
- 1663 Smol, J. P., and Douglas, M. S. V.: Crossing the final ecological threshold in high Arctic ponds,
1664 *Proceedings of the National Academy of Sciences of the United States of America*, 104, 12395-
1665 12397, 10.1073/pnas.0702777104, 2007.
- 1666 Sobakina, I., and Solomonov, N.: To the study of zooplankton of Lake Bolshoe Toko, *International*
1667 *Journal of applied and fundamental research*, 8, 180-182, 2013.
- 1668 Sokal, R., and Rohlf, F.: *Biometry: The Principles and Practice of Statistics in Biological Research*,
1669 W. H. Freeman and Co, New York, 1995.
- 1670 Solovieva, N., Klimaschewski, A., Self, A. E., Jones, V. J., Andrén, E., Andreev, A. A., Hammarlund,
1671 D., Lepskaya, E. V., and Nazarova, L.: The Holocene environmental history of a small coastal lake
1672 on the north-eastern Kamchatka Peninsula, *Global and Planetary Change*, 134, 55-66, 2015.
- 1673 Specziar, A., Arva, D., Toth, M., Mora, A., Schmera, D., Varbiro, G., and Eros, T.: Environmental and
1674 spatial drivers of beta diversity components of chironomid metacommunities in contrasting freshwater
1675 systems, *Hydrobiologia*, 819, 123-143, 10.1007/s10750-018-3632-x, 2018.
- 1676 Stewart, K. A., and Lamoureux, S. F.: Seasonal and microhabitat influences on diatom assemblages
1677 and their representation in sediment traps and surface sediments from adjacent High Arctic lakes:
1678 Cape Bounty, Melville Island, Nunavut, *Hydrobiologia*, 683, 265-286, 10.1007/s10750-011-0965-0,
1679 2012.
- 1680 Stief, P., Nazarova, L., and de Beer, D.: Chimney construction by *Chironomus riparius* larvae in
1681 response to hypoxia: microbial implications for freshwater sediments, *Journal of the North American*
1682 *Benthological Society*, 24, 858-871, 2005.
- 1683 Stoof-Leichsenring, K., Dulias, K., Biskaborn, B., Pestryakova, L., and Herzs Schuh, U.: Lake-depth
1684 related pattern of genetic and morphological diatom diversity in boreal Lake Bolshoe Toko, Eastern
1685 Siberia, *Biodiversity Research*, in review.
- 1686 Subetto, D. A., Nazarova, L. B., Pestryakova, L. A., Strykh, L. S., Andronikov, A. V., Biskaborn, B.,
1687 Diekmann, B., Kuznetsov, D. D., Sapelko, T. V., and Grekov, I. M.: Paleolimnological studies in
1688 Russian northern Eurasia: A review, *Contemporary Problems of Ecology*, 10, 327-335,
1689 10.1134/s1995425517040102, 2017.
- 1690 Swann, G. E. A., Leng, M. J., Sloane, H. J., Maslin, M. A., and Onodera, J.: Diatom oxygen isotopes:
1691 Evidence of a species effect in the sediment record, *Geochemistry Geophysics Geosystems*, 8,
1692 10.1029/2006gc001535, 2007.
- 1693 Strykh, L. S., Nazarova, L. B., Herzs Schuh, U., Subetto, D. A., and Grekov, I. M.: Reconstruction of
1694 palaeoecological and palaeoclimatic conditions of the Holocene in the south of the Taimyr according
1695 to an analysis of lake sediments, *Contemporary Problems of Ecology*, 10, 363-369,
1696 10.1134/s1995425517040114, 2017.

- 1697 ter Braak, C. J. F., and Prentice, I. C.: A theory of gradient analysis, in: *Advances in ecological*
1698 *research*, Elsevier, 271-317, 1988.
- 1699 ter Braak, C. J. F.: *Ordination*, in: *Data analysis in community and landscape ecology*, Cambridge
1700 University Press, 91-274, 1995.
- 1701 ter Braak, C. J. F., and Šmilauer, P.: *Canoco reference manual and user's guide: software for*
1702 *ordination*, version 5.0, Microcomputer power, 2012.
- 1703 Tjallingii, R., Rohl, U., Kolling, M., and Bickert, T.: Influence of the water content on X-ray
1704 fluorescence core-scanning measurements in soft marine sediments, *Geochemistry Geophysics*
1705 *Geosystems*, 8, Q02004
1706 10.1029/2006gc001393, 2007.
- 1707 Valiranta, M., Weckstrom, J., Siitonen, S., Seppa, H., Alkio, J., Juutinen, S., and Tuittila, E. S.:
1708 Holocene aquatic ecosystem change in the boreal vegetation zone of northern Finland, *Journal of*
1709 *Paleolimnology*, 45, 339-352, 10.1007/s10933-011-9501-5, 2011.
- 1710 Vemeaux, V., and Aleya, L.: Spatial and temporal distribution of chironomid larvae (Diptera:
1711 Nematocera) at the sediment—water interface in Lake Abbaye (Jura, France), in: *Oceans, Rivers*
1712 *and Lakes: Energy and Substance Transfers at Interfaces*, Springer, 169-180, 1998.
- 1713 Virgo, D.: Partition of Strontium between Coexisting K-Feldspar and Plagioclase in Some
1714 Metamorphic Rocks, *The Journal of Geology*, 76, 331-346, 10.1086/627332, 1968.
- 1715 Vogel, H., Wessels, M., Albrecht, C., Stich, H. B., and Wagner, B.: Spatial variability of recent
1716 sedimentation in Lake Ohrid (Albania/Macedonia), *Biogeosciences*, 7, 3333-3342, 2010.
- 1717 Voigt, C.: Data report: semiquantitative determination of detrital input to ACEX sites based on bulk
1718 sample X-ray diffraction data, in: *Proceedings of the Integrated Ocean Drilling Program, Volume 302*,
1719 edited by: Backman, J., Moran, K., McInroy, D.B., Mayer, L.A., and the Expedition 302 Scientists,
1720 Edinburgh, 2009.
- 1721 Walker, I. R., and Mathewes, R. W.: Early postglacial chironomid succession in southwestern British
1722 Columbia, Canada, and its paleoenvironmental significance, in: *Paleolimnology and the*
1723 *Reconstruction of Ancient Environments*, Springer, 147-160, 1990.
- 1724 Walker, I. R., Levesque, A. J., Cwynar, L. C., and Lotter, A. F.: An expanded surface-water
1725 palaeotemperature inference model for use with fossil midges from eastern Canada, *Journal of*
1726 *Paleolimnology*, 18, 165-178, 1997.
- 1727 Wang, L., Rioual, P., Panizzo, V. N., Lu, H., Gu, Z., Chu, G., Yang, D., Han, J., Liu, J., and Mackay,
1728 A. W.: A 1000-yr record of environmental change in NE China indicated by diatom assemblages from
1729 maar lake Erlongwan, *Quaternary Research*, 78, 24-34, 10.1016/j.yqres.2012.03.006, 2012a.
- 1730 Wang, Q., Yang, X. D., Hamilton, P. B., and Zhang, E. L.: Linking spatial distributions of sediment
1731 diatom assemblages with hydrological depth profiles in a plateau deep-water lake system of
1732 subtropical China, *Fottea*, 12, 59-73, 2012b.
- 1733 Wang, R., Zhang, Y., Wuennemann, B., Biskaborn, B. K., Yin, H., Xia, F., Zhou, L., and Diekmann,
1734 B.: Linkages between Quaternary climate change and sedimentary processes in Hala Lake, northern
1735 Tibetan Plateau, China, *Journal of Asian Earth Sciences*, 107, 140-150,
1736 10.1016/j.jseaes.2015.04.008, 2015.
- 1737 Weltje, G. J., and Tjallingii, R.: Calibration of XRF core scanners for quantitative geochemical logging
1738 of sediment cores: Theory and application, *Earth and Planetary Science Letters*, 274, 423-438,
1739 10.1016/j.epsl.2008.07.054, 2008.

- 1740 Wiederholm, T.: Chironomidae of Holarctic region: keys and diagnoses. Part 1, *Larvae Entomol*
 1741 *Scand Suppl*, 19, 1-457, 1983.
- 1742 Wischniewski, J., Mackay, A. W., Appleby, P. G., Mischke, S., and Herzsuh, U.: Modest diatom
 1743 responses to regional warming on the southeast Tibetan Plateau during the last two centuries,
 1744 *Journal of Paleolimnology*, 46, 215-227, 10.1007/s10933-011-9533-x, 2011.
- 1745 Wolfe, A.: Spatial patterns of modern diatom distribution and multiple paleolimnological records from
 1746 a small arctic lake on Baffin Island, Arctic Canada, *Canadian Journal of Botany-Revue Canadienne*
 1747 *De Botanique*, 74, 435-449, 1996.
- 1748 Yang, H., Flower, R. J., and Battarbee, R. W.: Influence of environmental and spatial variables on the
 1749 distribution of surface sediment diatoms in an upland loch, Scotland, *Acta Botanica Croatica*, 68,
 1750 367-380, 2009.
- 1751 Yang, L. W., Chen, S. Y., Zhang, J., Yu, S. Y., and Deng, H. G.: Environmental factors controlling the
 1752 spatial distribution of subfossil Chironomidae in surface sediments of Lake Dongping, a warm
 1753 temperate lake in North China, *Environmental Earth Sciences*, 76, 10.1007/s12665-017-6858-4,
 1754 2017.
- 1755 Zhao, Y., Sayer, C. D., Birks, H. H., Hughes, M., and Peglar, S. M.: Spatial representation of aquatic
 1756 vegetation by macrofossils and pollen in a small and shallow lake, *Journal of Paleolimnology*, 35,
 1757 335-350, 10.1007/s10933-005-1336-5, 2006.
- 1758 Zhirkov, I., Trofimova, T., Zhirkov, K., Pstryakova, L., Sobakina, I., and Ivanov, K.: Current
 1759 geoecological state of Lake Bolshoe Toko, *International Journal of applied and fundamental*
 1760 *research*, 8, 208-213, 2016.
- 1761 Zinchenko, T. D., Gladyshev, M. I., Makhutova, O. N., Sushchik, N. N., Kalachova, G. S., and
 1762 Golovatyuk, L. V.: Saline rivers provide arid landscapes with a considerable amount of biochemically
 1763 valuable production of chironomid (Diptera) larvae, *Hydrobiologia*, 722, 115-128, 2014.
 1764